

Forschungszentrum Karlsruhe
Technik und Umwelt

Wissenschaftliche Berichte
FZKA 6320

Characteristic Current Degradation of Commercial NbTi-Multifilamentary Superconductors due to Annealing

W. Maurer, H. Münch, Th. Schneider, C. Ruf
Institut für Technische Physik

Juli 1999



Forschungszentrum Karlsruhe

Technik und Umwelt

Wissenschaftliche Berichte

FZKA 6320

Characteristic current degradation of commercial NbTi-multifilamentary
superconductors due to annealing

W. Maurer, H. Münch*, Th. Schneider, C. Ruf

Institut für Technische Physik

*Max-Planck-Institut für Plasmaphysik, Garching

Forschungszentrum Karlsruhe GmbH, Karlsruhe
1999

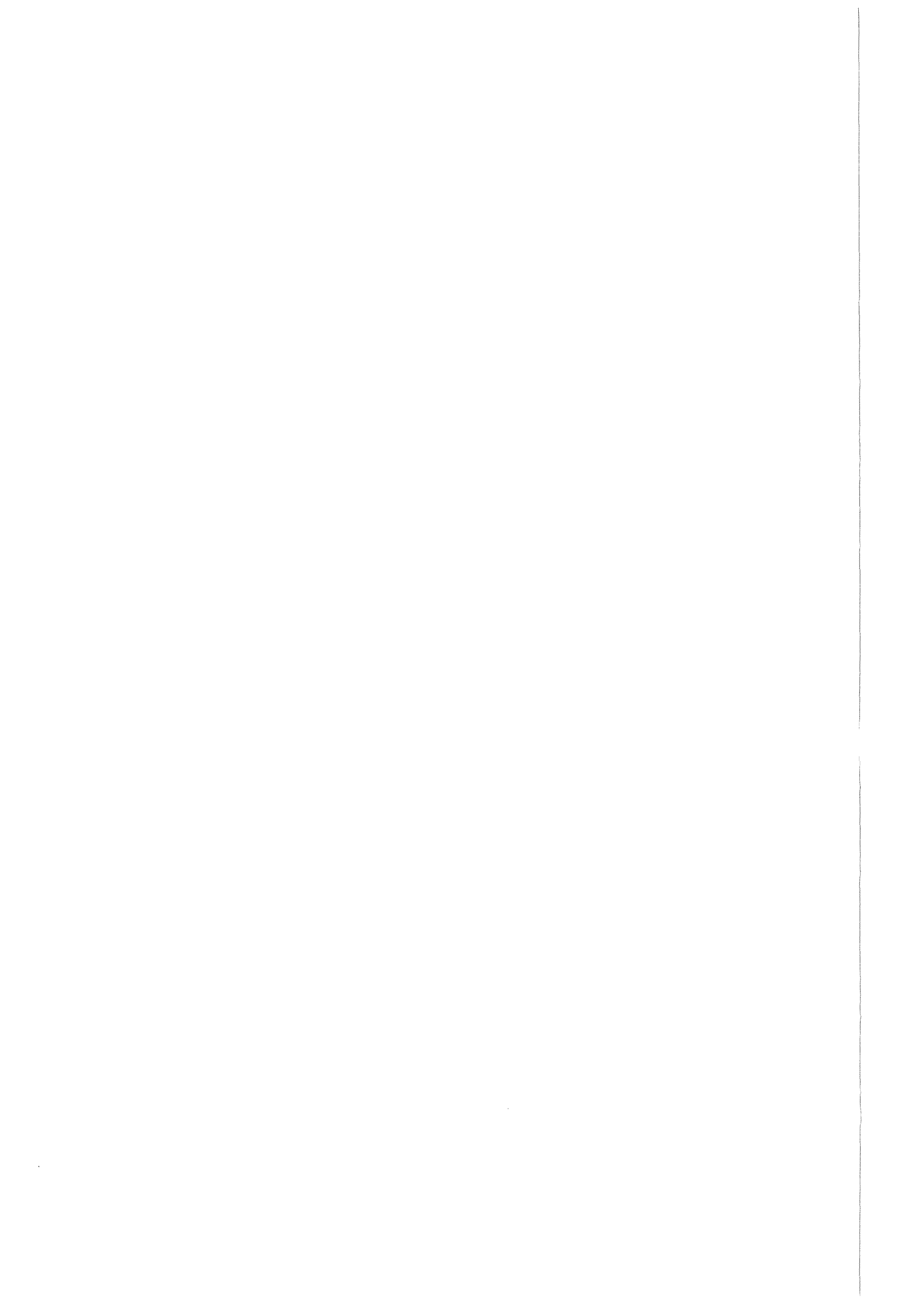
Als Manuskript gedruckt
Für diesen Bericht behalten wir uns alle Rechte vor
Forschungszentrum Karlsruhe GmbH
Postfach 3640, 76021 Karlsruhe
Mitglied der Hermann von Helmholtz-Gemeinschaft
Deutscher Forschungszentren (HGF)
ISSN 0947-8620

In the framework of the development of superconducting coils for the stellarator physics experiment Wendelstein 7-X (W 7-X) the reduction of the critical current, better defined as characteristic current due to annealing was investigated. The characteristic current level was defined using the $0.1 \mu\text{V}/\text{cm}$ criterion. The technical superconductor for the magnets of this experiment is a cable-in-conduit conductor with a co-extruded Al-alloy jacket. During the co-extrusion of this jacket onto the superconducting cable heat influx to the NbTi-strands occurs. This is also true for subsequent working steps like welding, brazing, and soldering. Therefore, a degradation of the characteristic current is expected for optimized NbTi-strands. In order to clarify the behaviour of the NbTi-strands at temperatures which occur during the co-extrusion process and/or the working steps mentioned above a study was performed where the annealing temperature and annealing time was varied, the temperature up to $600 \text{ }^\circ\text{C}$ and the time up to 120 s. The NbTi multifilamentary superconductor is commercially available. The results of the measurements of the characteristic current at 4.2 K in the field range from 2 T to 10 T are presented. A generalization of the results is made in order to point out the tendencies of the degradation of the characteristic current. These results were used to predict the behaviour of the W 7-X conductor cable itself.

Degradation des charakteristischen Stromes von kommerziell verfügbaren NbTi-Multifilamentsupraleitern aufgrund von Wärmebehandlung

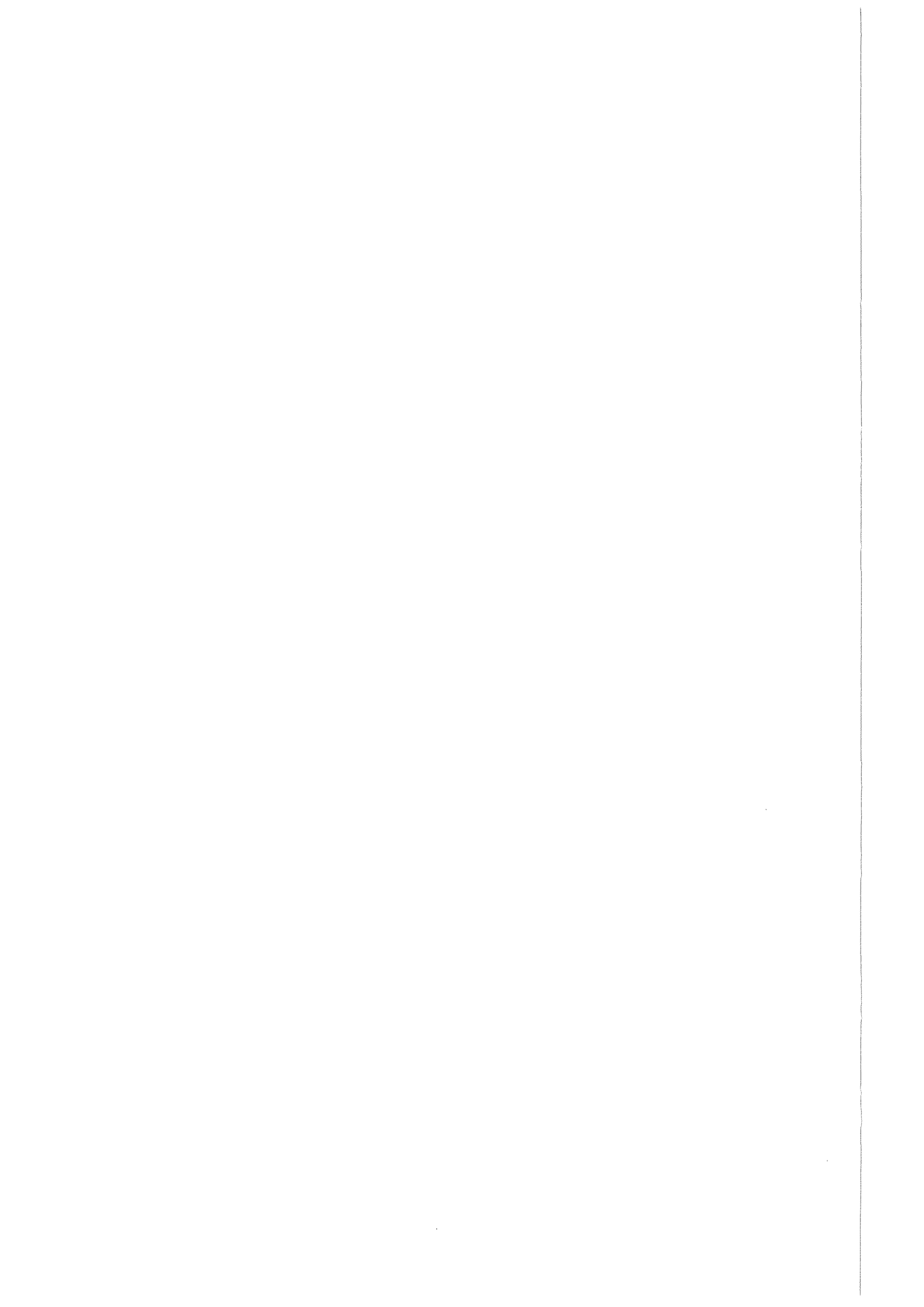
Zusammenfassung:

Im Zusammenhang mit der Entwicklung supraleitender Spulen für das Stellarator Physikexperiment Wendelstein 7-X (W 7-X) wurde die Reduktion des kritischen Stromes, besser definiert als charakteristischer Strom aufgrund von Wärmebehandlung, untersucht. Der charakteristische Strom wurde mit Hilfe des $0.1 \mu\text{V}/\text{cm}$ Kriteriums definiert. Der technische Supraleiter für die Magnete von W 7-X ist ein innengekühlter Kabelleiter mit einer koextrudierten Hülle aus einer Aluminiumverbindung. Während der Koextrusion dieser Hülle auf das supraleitende Kabel tritt Erwärmung der NbTi Drähte auf. Dies gilt auch für darauffolgende Arbeitsschritte wie Schweißen, Hart- und Weichlöten. Aufgrund dieser Erwärmung ist eine Degradation des charakteristischen Stromes für optimierte NbTi Drähte zu erwarten. Um diesen Sachverhalt zu klären, wurde eine Studie durchgeführt, bei der die Temperatur bei der Wärmebehandlung bis zu $600 \text{ }^\circ\text{C}$ und die Zeit bis zu 120 s variiert wurde. Der NbTi Multifilamentdraht ist kommerziell erhältlich. In diesem Bericht werden die Ergebnisse der Messungen des charakteristischen Stromes bei 4,2 K im Feldbereich von 2 T bis 10 T vorgestellt. Eine Verallgemeinerung der Resultate wurde gemacht, um das tendenzielle Verhalten der Degradation des charakteristischen Stromes aufzuzeigen. Diese Resultate wurden benutzt, um das Verhalten des W 7-X Kabels vorauszusagen.



Contents

1. Introduction	1
2. Annealing behaviour of a commercially available strand (Swissmetal)	5
2.1 Description of superconductive strand	5
2.2 Preparation of samples	6
2.3 Measurement conditions and procedure	7
2.4 Measurement results	9
2.5 Evaluation of test results	11
2.6 Generalization	31
3. Application to the W 7-X conductor cable	39
3.1 Description of superconductor	39
3.2 Application to the W 7-X conductor cable	41
4. Summary and conclusion	43



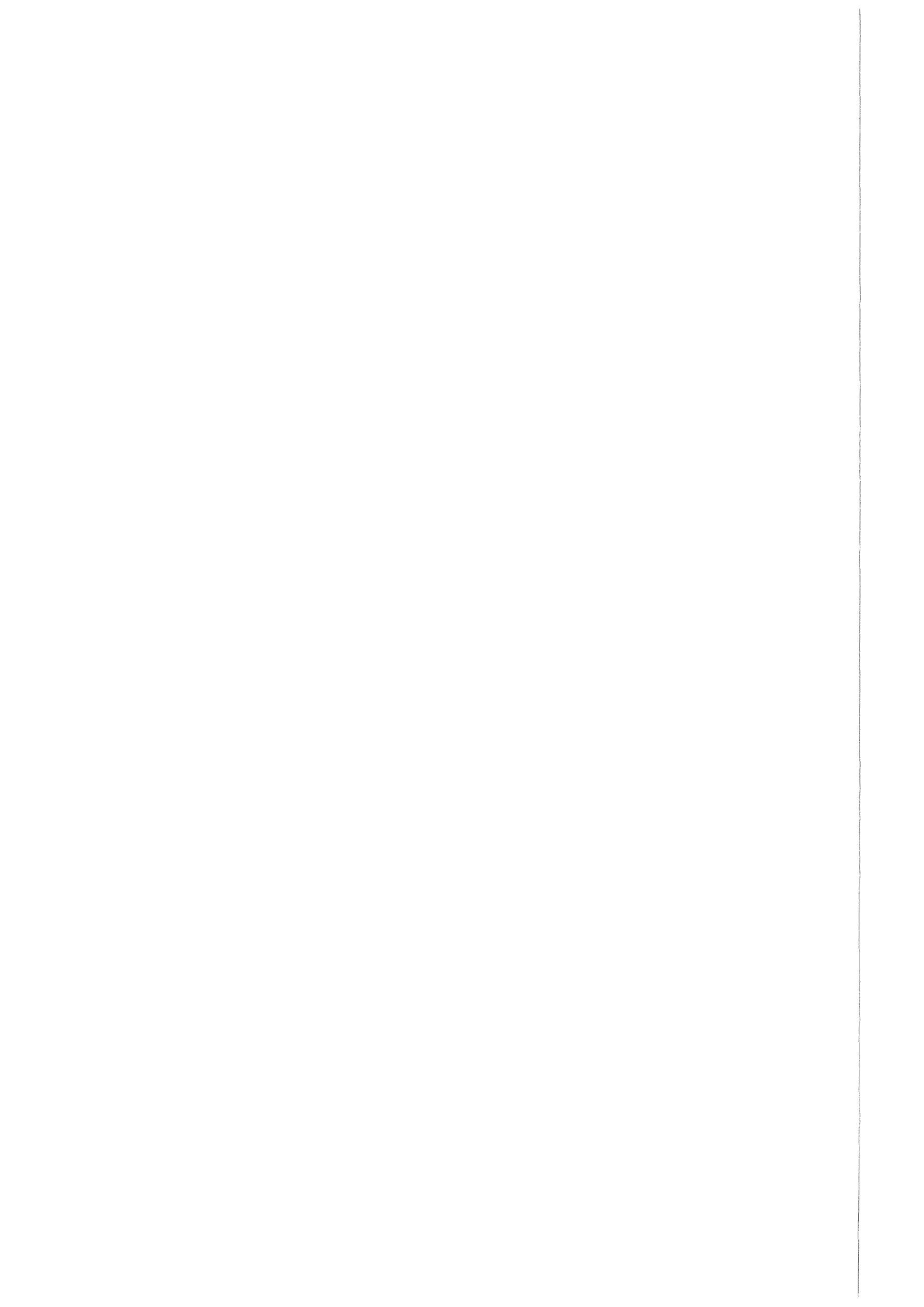
Figures

1.	Sample prepared for the measurement	7
2.	Typical log (Electric field) vs current characteristic	8
3.	Characteristic current vs magnetic field	14
4.	Characteristic current vs magnetic field	14
5.	Characteristic current vs magnetic field	15
6.	Characteristic current vs magnetic field	15
7.	Characteristic current vs magnetic field	17
8.	Characteristic current vs magnetic field	17
9.	Characteristic current vs magnetic field	18
10.	Characteristic current vs annealing time for 2 T	20
11.	Characteristic current vs annealing time for 3 T	20
12.	Characteristic current vs annealing time for 4 T	21
13.	Characteristic current vs annealing time for 5 T	21
14.	Characteristic current vs annealing time for 6 T	22
15.	Characteristic current vs annealing time for 7 T	22
16.	Characteristic current vs annealing time for 8 T	23
17.	Characteristic current vs annealing time for 9 T	23
18.	Characteristic current vs annealing time for 10 T	24
19.	Characteristic current vs annealing temperature for 2 T	26
20.	Characteristic current vs annealing temperature for 3 T	26
21.	Characteristic current vs annealing temperature for 4 T	27
22.	Characteristic current vs annealing temperature for 5 T	27
23.	Characteristic current vs annealing temperature for 6 T	28
24.	Characteristic current vs annealing temperature for 7 T	28
25.	Characteristic current vs annealing temperature for 8 T	29
26.	Characteristic current vs annealing temperature for 9 T	29
27.	Characteristic current vs annealing temperature for 10 T	30
28.	Normalized current vs annealing time	33
29.	Normalized current vs annealing time	33
30.	Normalized current vs annealing time	34
31.	Normalized current vs annealing temperature	36
32.	Normalized current vs annealing temperature	36
33.	Normalized current vs annealing temperature	37
34.	Technical superconductor (LMI) for W 7-X	40
35.	Histogram for the critical current, annealing time and temperature for 2T	44



Tables

1.	Differences of the two conductor classes using Al material	1
2.	Characteristic data of the strand material [24]	5
3.	Annealing conditions of the samples	6
4.	Main characteristics of the measurement.	8
5.	Characteristic current of all samples	10
6.	Normalized characteristic current of all samples	32
7.	Characteristic data of the LMI superconductor [25]	39
8.	Application to the 16 kA cable	41



Abbreviations

Abbreviation	Meaning
CIC	Cable-in-conduit
CICC	Cable-in-conduit conductor
EM-LMI	EUROPA METALLI - LA METALLI INDUSTRIALE
LHD	Large Helical Device (plasma physics stellarator experiment)
RRR	Residual resistivity ratio
SC or Sc	Superconductor or superconductive or superconducting
TCCC	Transport current carrying capacity
W 7-X	Wendelstein 7-X (plasma physics stellarator experiment)

1. Introduction

Wendelstein 7-X (W 7-X) is a large plasma stellarator physics experiment which is currently built in Germany [1]. The coils of this experiment are superconductive. In the case of the magnet system of the advanced modular stellarator Wendelstein 7-X the requirements on the conductor properties are governed essentially by mechanical properties [2]. Primary goal was the development of a flexible conductor which can be wound into the nonplanar shape of a modular coil. The solution chosen is a cable-in-conduit (CIC) conductor with an aluminium jacket which is co-extruded or produced by a conform process. This co-extrusion or conform process takes place at a temperature of about 525 °C. During this process heat influx to the strands occurs. Also, during the fabrication of the superconductor and the coil, production processes like cabling, rolling, soldering, brazing, and welding are necessary. This leads also to heat influx to the superconducting strands.

It is common knowledge that the transport current carrying capability (TCCC) of NbTi superconductors is optimized in a very sophisticated procedure between cold-work and heat treatment [3,4,5,6,7,8]. The latter is done, in general, at temperatures between 350 and 400 °C. Once optimized, an additional heat treatment, however, or an unintentional overheating influences the superconducting properties [9,10]. In general, the TCCC degrades. Therefore, a degradation of the TCCC of the Wendelstein 7-X superconductor is expected due to the possible heat influx mentioned above. The question arises which heat treatments are tolerable without too severe a degradation of the critical current, better defined as **characteristic current of the superconductor**. This notion is used throughout this report. **The characteristic current level was defined using the 0.1 $\mu\text{V}/\text{cm}$ criterion.**

There is a large experience with superconductors stabilized with aluminium going back to the early seventies [11,12]. Especially in the field of detectors in particle physics, a great deal of experience is available [13,14,15]. However, the aluminium-stabilized conductors for detectors or even a stellarator (Large Helical Device) [16], are different from the conductor used for W 7-X. These differences of the two conductor classes are listed in Table 1.

Property	Aluminium-stabilized conductor	W 7-X stellarator conductor
Type	Monolithic	Cable-in-conduit
Kind of Al	High purity Al	Al-alloy
Purpose	Electrical stability	Mechanical stability
RRR	Several hundred	2 - 3
Al or Cu to Sc ratio	High(> 10) (Al)	Low(\sim 2) (Cu)
Cable	Soldered Rutherford	Transparent for Helium
Fabrication of jacket	Co-extrusion	Co-extrusion or conform process
Temperature of co-extrusion	\sim 400 °C	\sim 500 °C
Desired quality of bond cable/jacket	Strong	Weak
Cooling	Pool boiling, Indirect	Internal

Several authors report a degradation of the superconductor after the fabrication [17,18,19,20,21,22,23]. It is the consequence and the combined effect of the cabling of the strands and the extrusion or conform process. A degradation of the transport current carrying capability (TCCC) of an optimized NbTi superconductor is generally expected beyond 200°C [6,20]. The degradation strongly depends on the temperature level and the time of annealing.

In [17], the production of the DELPHI conductor is described. A high-purity aluminium jacket is co-extruded around a Rutherford cable. The extrusion temperature, extrusion time, and stop durations were kept at a level that the characteristic current of the NbTi-superconductor is not degraded below the specified value. Final performance tests showed that the total degradation was at no more than 13 %.

In [18], the degradation of the DELPHI conductor is shown as a result of a systematic annealing of the conductor. The annealing temperatures were 350 °C, 375 °C, and 400 °C and the annealing times 1.5 min, 3 min, 6 min, and 12 min. At the worst combination (400 °C and 12 min) the degradation of the characteristic current was less than 12 %.

In [19], the aluminium stabilized superconductor for the ALEPH solenoid is described. Aluminium is continuously co-extruded around a Cu/NbTi-cable at a temperature of about 450 °C. At 2 T a degradation of the characteristic current of < 4 % was observed which is tolerable.

In [20], the aluminium stabilized superconductor for the ZEUS thin solenoid is described. Samples of the basic strand for the Rutherford cable have been heated in a range of temperatures and time pertinent to the scheduled production process. The tests have shown that the characteristic current decreases at annealing temperatures above 200 °C. Tests on the final composite conductor at 5.8 T showed a characteristic current degradation of 35 % due to the fabrication. It was found that a certain amount of the basic strand have been broken but the major source of the observed degradation is the heat treatment performed on the NbTi strands before and during the co-extrusion process. The pre-heating is necessary in order to prevent the chilling effect on the cladding material, and the heating during co-extrusion is unavoidable. Measurements on basic strands taken from a Rutherford cable subjected to the pre-extrusion heating showed an additional 8 % decrease of the characteristic current.

In [21,22], the development of aluminium clad superconductors is described, and a characterization is given. Samples of multifilamentary Cu/NbTi-wires with varying thicknesses of the aluminium cladding were used with final outer diameters of 3 mm, 4 mm, and 5 mm. Co-extrusion temperatures have been varied from 365 °C to 450 °C, and the extrusion speed ranged from 15 m/min to over 80 m/min. No effect on the characteristic current has been found explainable by the very short residence times which the superconductive core is actually in contact with the hot aluminium.

These results prove that one has to compromise between a good metallurgical bonding between aluminium and the Rutherford cable and the attainable current density. Also apparent is the strong influence of the annealing temperature, the annealing time, and the co-extrusion speed.

The aim of the investigation presented here is to study the annealing behaviour of a commercially available superconductive strand at high annealing temper-

ature and to apply the results to cable-in-conduit conductors. The experimental conditions are:

- Measurement temperature: 4.2 K
- Full scale magnetic field range for NbTi, i.e., up to 10 T
- Annealing temperature: 400 °C, 500 °C, 550 °C, and 600 °C
- Annealing times: 10 s, 30 s, and 120 s (according to the practical experience)

The data achieved were generalized and applied in order to predict the performance of the W 7-X conductor cable.

2. Annealing behaviour of a commercially available strand (Swissmetal)

The goal of this investigation was to get information for the practically working engineer about the annealing behaviour of a commercially available strand material during the fabrication of a technical superconductor and the confectioning of superconductive coils. It should give a help and rules for the engineer in the workshop.

It is not the aim to explain the metallurgical behaviour.

2.1 Description of superconductive strand

A commercially available strand was chosen as candidate for an annealing study of the expected degradation. The characteristics are given in Table 2. The strand was chosen by chance because it was available as surplus.

Table 2. Characteristic data of the strand material [24]	
Parameter	Values
Manufacturer	Swissmetal, Dornach, Switzerland
Strand type	S-48
Diameter of strand	0.58 mm
Superconducting material	Nb 47 wt % Ti
Matrix material	Cu
Ratio Cu/NbTi	2.14 : 1
Filament number	48
Filament diameter	$\leq 50 \mu\text{m}$
Twist pitch	25 mm
Weight	2.12 g/m
Length	Up to several km
Residual resistivity ratio RRR	> 100
Magnetic field B	Critical current I_{c0} (taken from picture on data sheet)
1 T	715 A
2 T	495 A
3 T	396 A
4 T	325 A
5 T	265 A
6 T	210 A
7 T	155 A
8 T	105 A

2.2 Preparation of samples

From a practical viewpoint a temperature region up to 600 °C and a time scale up to 120 s was chosen for the annealing conditions. The annealing temperatures are 400°C, 500°C, 550°C, and 600°C, and the annealing times are 10 s, 30 s, and 120 s. The heat treatment for the NbTi strands which simulates the conditions during the production steps mentioned above were performed at the IPP Garching. The treatment of the samples is shown in Table 3 on page 6.

Sample number	Temperature (°C)	Time of heat treatment (s)
1	as delivered	no heat treatment
2	400	10
3	400	30
4	400	120
5	500	10
6	500	30
7	500	120
8	550	10
9	550	30
10	550	120
11	600	10
12	600	30
13	600	120

The arrangement for the heat treatment was the following. The strand was inserted into the grooves of two plates of stainless steel over a length of about 105 mm. Both plates were heated by a gas flame to the required temperature measured by a contact thermometer. The decrease of the temperature during the maximum measurement time was about 10 °C. For shorter times it was negligible. The accuracy of the temperature measurement is estimated to be ± 5 °C. The annealed zone of 105 mm length is in the middle of the 2.5 m long sample. Figure 1 on page 7 shows a picture of samples prepared for the measurement.



Figure 1. Sample prepared for the measurement.

The sample was wound into a helical form onto a copper/G10/copper sample holder at a pitch of 1 mm. The wire was soldered in the copper regions and further restrained by the use of stycast. Voltage taps were soldered across the length of the annealed conductor.

2.3 Measurement conditions and procedure

The main characteristics of the measurement are given in Table 4 on page 8.

Table 4. Main characteristics of the measurement.	
Parameter	Values
Number of samples	3 x 4 = 12 (+ 1 without annealing)
Test temperature	4.2 K
Test magnetic field	Up to 10 T from 2 T in steps of 1 T
Test current	Up to 500 A (3000 A) depending on testing rig and sample
Test cryostat	Bath cooled with insert for samples
Shape of sample	Spiral on sample holder ($\varnothing = 33.3$ mm or 90 mm)
Length of sample	2.5 m minimum
Total number of turns	15
Length of heat treated zone	One turn of 105 mm (ideal)
Location of heat treated zone	In the middle of the sample (to be seen by the temper colour)

The voltage vs current characteristic for the measurement of the characteristic current was obtained by using a new method. The sample current was increased in steps. It was constant during the period of the voltage measurements in order to exclude any noise voltage. All measurements reported here were performed at 4.2 K with the external field perpendicular to the conductor. The characteristic current level was defined using the $0.1 \mu\text{V}/\text{cm}$ criterion. In all measurements, no effects due to degradation or damage by strain or movements were observed. Figure 2 shows an example of the voltage vs current characteristic.

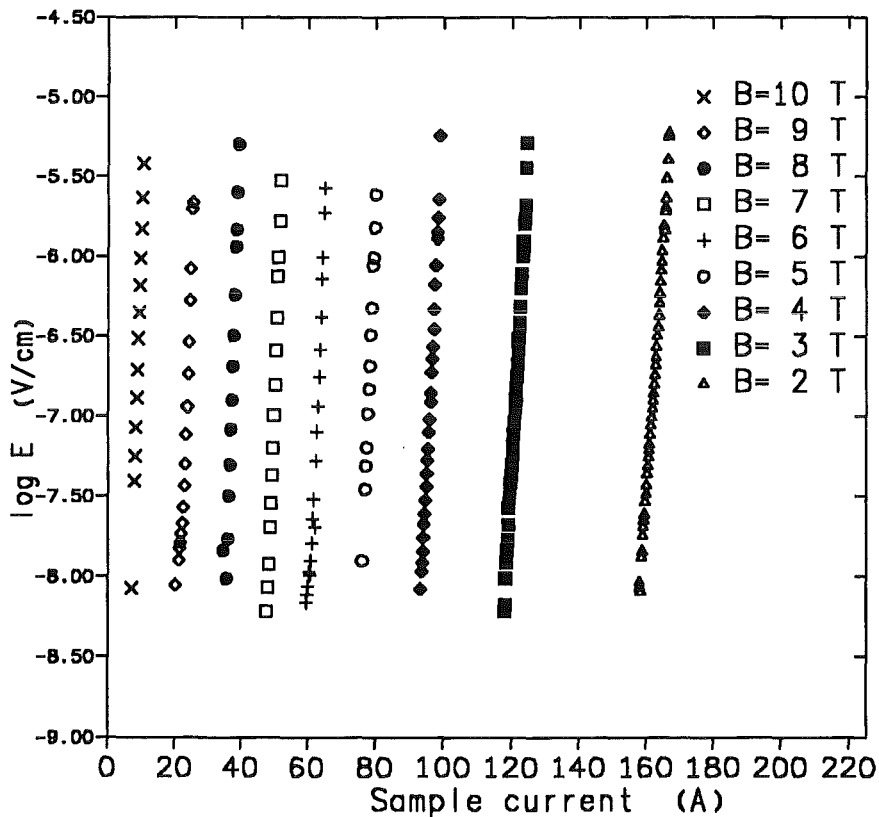


Figure 2. Typical log (Electric field) vs current characteristic.

2.4 Measurement results

The results of the measurements are collected in Table 5 on page 10

Table 5. Characteristic current of all samples													
Characteristic current $I_{ca}(B)$ in [A] at annealing temperature and annealing time													
Annealing temperature →		400 °C			500 °C			550 °C			600 °C		
Annealing time	→	10 s	30 s	120 s	10 s	30 s	120 s	10 s	30 s	120 s	10 s	30 s	120 s
B [T]	No an-nealing												
2	461.3	440.1	419.1	402.1	426.0	372.7	235.5	263.2	161.5	92.0	113.9	49.7	-
3	369.1	351.6	332.4	315.3	337.2	289.9	177.0	201.6	120.8	64.6	83.0	28.4	-
4	304.2	284.6	266.9	252.0	271.8	231.4	139.5	160.9	95.8	45.2	63.3	17.7	-
5	248.3	229.2	213.6	200.8	218.0	185.0	111.8	130.2	77.8	34.2	48.8	11.8	-
6	195.2	178.6	166.2	155.3	169.7	144.3	88.0	104.3	62.9	26.3	38.4	8.7	-
7	145.4	131.2	121.8	113.2	124.6	107.4	67.1	80.6	49.7	19.8	31.2	6.9	-
8	94.7	86.0	79.7	73.4	81.1	71.7	46.9	57.5	37.0	15.4	25.1	5.4	-
9	47.0	43.9	40.1	36.6	41.2	37.5	26.6	33.3	23.3	12.9	17.5	4.2	-
10	12.1	11.9	10.0	8.8	11.0	9.5	7.7	9.7	8.4	6.4	7.7	4.1	-

2.5 Evaluation of test results

The results of the measurement are given in the following figures. Different views are chosen in order to show the tendencies of the behaviour. They form groups in the following way:

- 1. I_c vs B for a certain annealing temperature and the annealing time as parameter**
- 2. I_c vs B for a certain annealing time and the annealing temperature as parameter**
- 3. I_c vs annealing time for a certain magnetic field and the annealing temperature as parameter**
- 4. I_c vs annealing temperature for a certain magnetic field and the annealing time as parameter**

The grouping of the figures is as follows:

To group 1:

Figure 3 on page 14: I_c vs B for an annealing temperature of 400 °C and the annealing time as parameter

Figure 4 on page 14: I_c vs B for an annealing temperature of 500 °C and the annealing time as parameter

Figure 5 on page 15: I_c vs B for an annealing temperature of 550 °C and the annealing time as parameter

Figure 6 on page 15: I_c vs B for an annealing temperature of 600 °C and the annealing time as parameter

To group 2:

Figure 7 on page 17: I_c vs B for an annealing time of 10 s and the annealing temperature as parameter

Figure 8 on page 17: I_c vs B for an annealing time of 30 s and the annealing temperature as parameter

Figure 9 on page 18: I_c vs B for an annealing time of 120 s and the annealing temperature as parameter

To group 3:

Figure 10 on page 20: I_c vs annealing time for 2 T and the annealing temperature as parameter

Figure 11 on page 20: I_c vs annealing time for 3 T and the annealing temperature as parameter

Figure 12 on page 21: I_c vs annealing time for 4 T and the annealing temperature as parameter

Figure 13 on page 21: I_c vs annealing time for 5 T and the annealing temperature as parameter

Figure 14 on page 22: I_c vs annealing time for 6 T and the annealing temperature as parameter

Figure 15 on page 22: I_c vs annealing time for 7 T and the annealing temperature as parameter

Figure 16 on page 23: I_c vs annealing time for 8 T and the annealing temperature as parameter

Figure 17 on page 23: I_c vs annealing time for 9 T and the annealing temperature as parameter

Figure 18 on page 24: I_c vs annealing time for 10 T and the annealing temperature as parameter

To group 4:

Figure 19 on page 26: I_c vs annealing temperature for 2 T and the annealing time as parameter

Figure 20 on page 26: I_c vs annealing temperature for 3 T and the annealing time as parameter

Figure 21 on page 27: I_c vs annealing temperature for 4 T and the annealing time as parameter

Figure 22 on page 27: I_c vs annealing temperature for 5 T and the annealing time as parameter

Figure 23 on page 28: I_c vs annealing temperature for 6 T and the annealing time as parameter

Figure 24 on page 28: I_c vs annealing temperature for 7 T and the annealing time as parameter

Figure 25 on page 29: I_c vs annealing temperature for 8 T and the annealing time as parameter

Figure 26 on page 29: I_c vs annealing temperature for 9 T and the annealing time as parameter

Figure 27 on page 30: I_c vs annealing temperature for 10 T and the annealing time as parameter

Figures of group 1

To group 1:

Figure 3 on page 14: I_c vs B for an annealing temperature of 400 °C and the annealing time as parameter

Figure 4 on page 14: I_c vs B for an annealing temperature of 500 °C and the annealing time as parameter

Figure 5 on page 15: I_c vs B for an annealing temperature of 550 °C and the annealing time as parameter

Figure 6 on page 15: I_c vs B for an annealing temperature of 600 °C and the annealing time as parameter

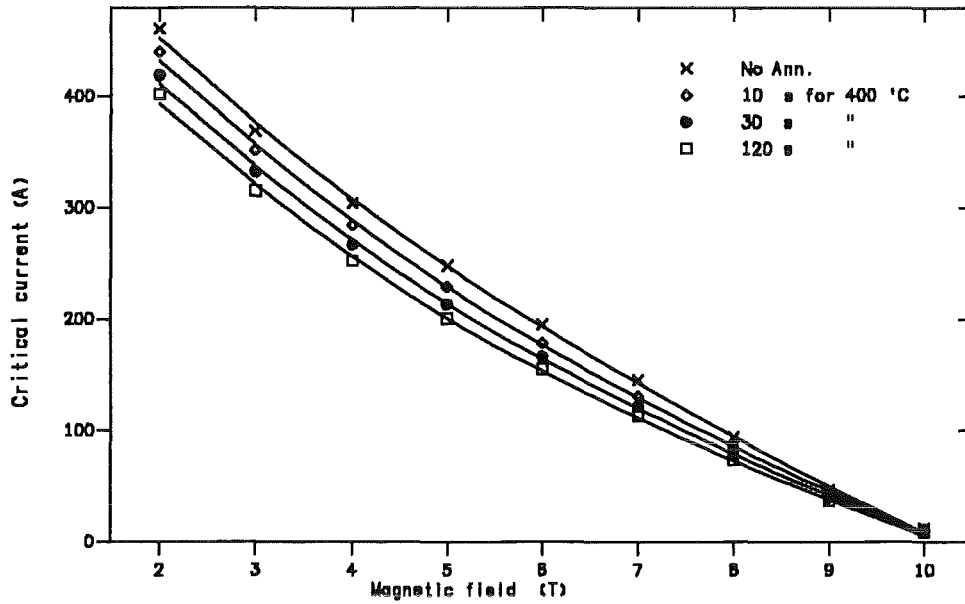


Figure 3. Characteristic current vs magnetic field. for an annealing temperature of 400 °C and the annealing time as parameter

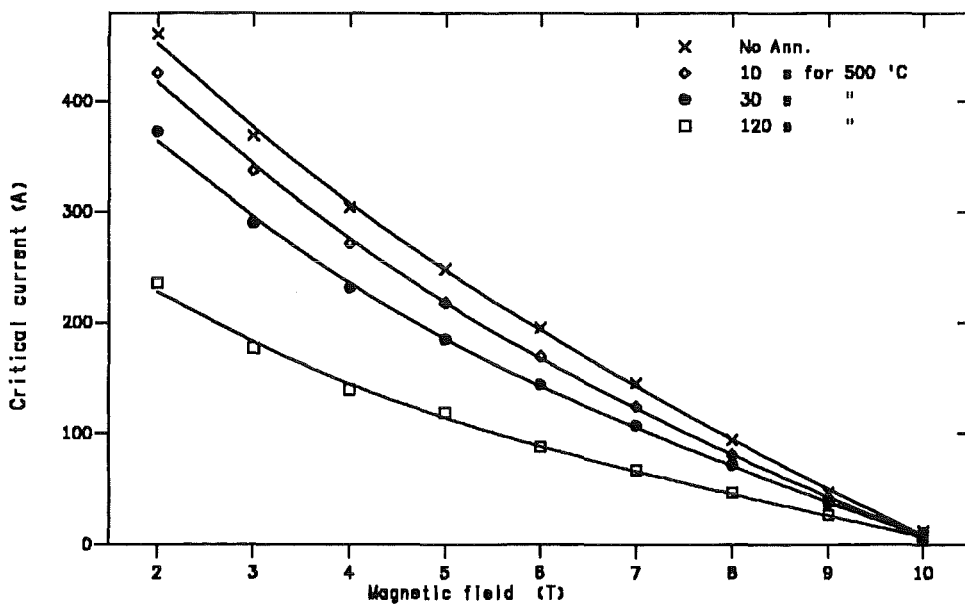


Figure 4. Characteristic current vs magnetic field. for an annealing temperature of 500 °C and the annealing time as parameter

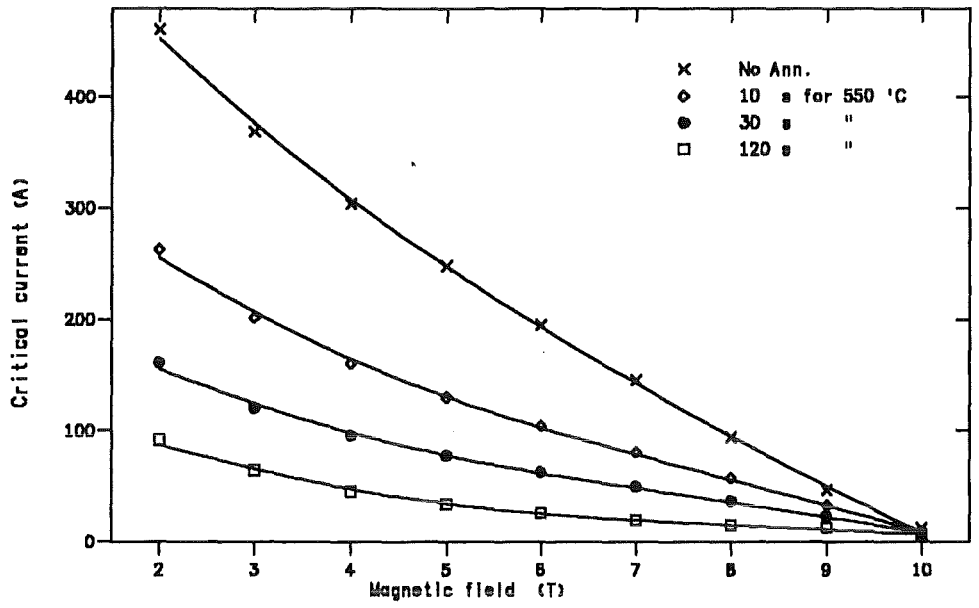


Figure 5. Characteristic current vs magnetic field. for an annealing temperature of 550 °C and the annealing time as parameter

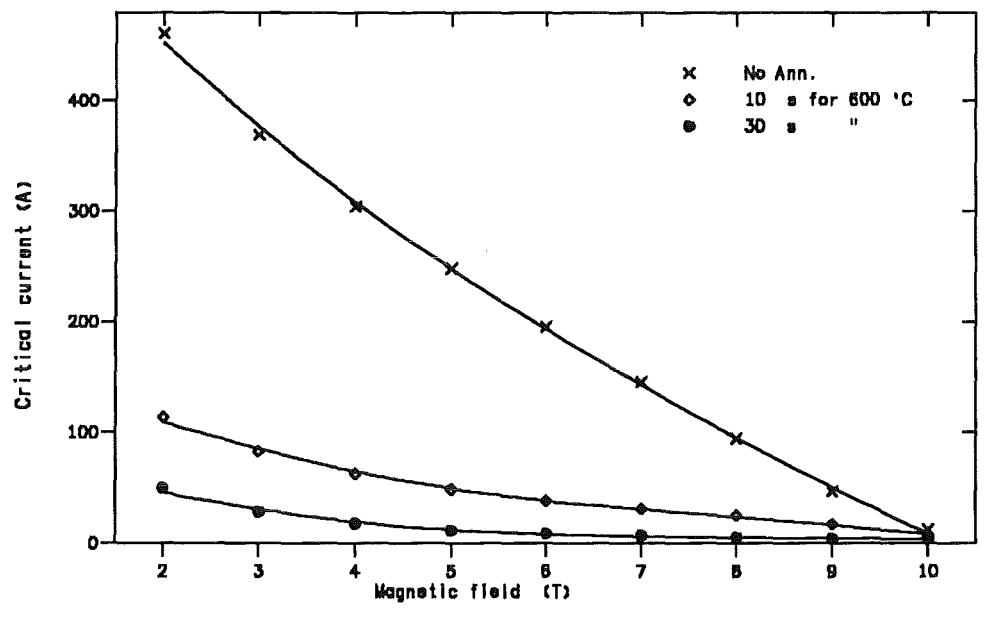


Figure 6. Characteristic current vs magnetic field. for an annealing temperature of 600 °C and the annealing time as parameter

Figures of group 2

To group 2:

Figure 7 on page 17: I_c vs B for an annealing time of 10 s and the annealing temperature as parameter

Figure 8 on page 17: I_c vs B for an annealing time of 30 s and the annealing temperature as parameter

Figure 9 on page 18: I_c vs B for an annealing time of 120 s and the annealing temperature as parameter

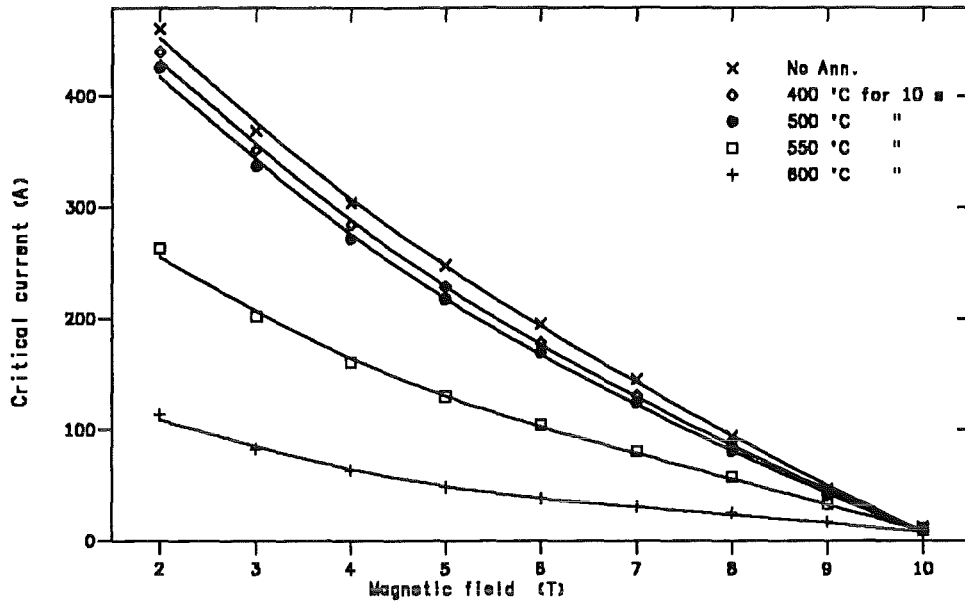


Figure 7. Characteristic current vs magnetic field. for an annealing time of 10 s and the annealing temperature as parameter

Figure 7 shows measured characteristic current curves vs the applied magnetic field for an annealing time of 10 s and for different temperature levels. A catastrophic deterioration of the transport current carrying capability (TCCC) occurs at temperatures > 550 °C even at ten seconds. However, the degradation for temperatures less than 500 °C lies in the range of only a few percent.

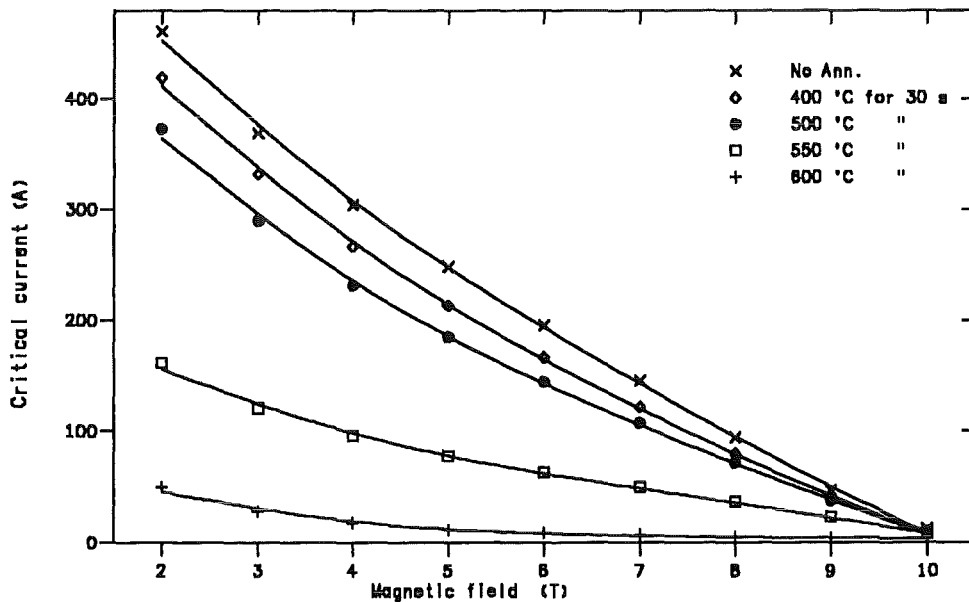


Figure 8. Characteristic current vs magnetic field. for an annealing time of 30 s and the annealing temperature as parameter

Figure 8 shows measured characteristic current curves vs the applied magnetic field for an annealing time of 30 s and for different temperature levels. A distinct splitting of the curves for $T < 500\text{ }^{\circ}\text{C}$ is the consequence of the three times longer annealing time. For temperatures $> 550\text{ }^{\circ}\text{C}$ the TCCC is only about one third of the initial ones.

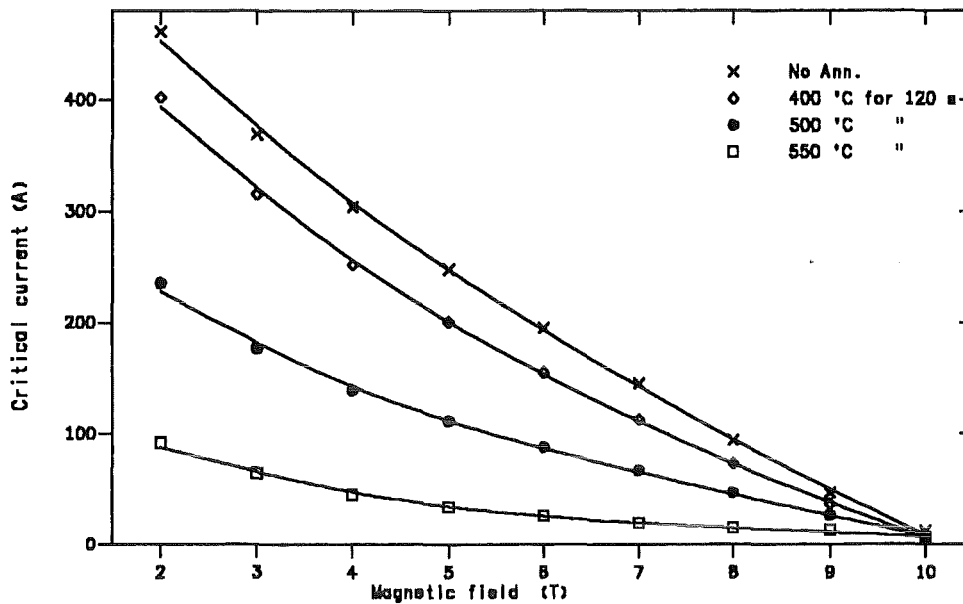


Figure 9. Characteristic current vs magnetic field. for an annealing time of 120 s and the annealing temperature as parameter

Figure 9 shows measured characteristic current curves vs the applied magnetic field for an annealing time of 120 s and for different temperature levels. Compared to Figure 7 on page 17 and Figure 8 on page 17 the catastrophic degradation of the TCCC starts between $400\text{ }^{\circ}\text{C}$ and $500\text{ }^{\circ}\text{C}$. For $600\text{ }^{\circ}\text{C}$ a nearly complete loss of the TCCC is found.

Figures of group 3

To group 3:

Figure 10 on page 20: I_c vs annealing time for 2 T and the annealing temperature as parameter

Figure 11 on page 20: I_c vs annealing time for 3 T and the annealing temperature as parameter

Figure 12 on page 21: I_c vs annealing time for 4 T and the annealing temperature as parameter

Figure 13 on page 21: I_c vs annealing time for 5 T and the annealing temperature as parameter

Figure 14 on page 22: I_c vs annealing time for 6 T and the annealing temperature as parameter

Figure 15 on page 22: I_c vs annealing time for 7 T and the annealing temperature as parameter

Figure 16 on page 23: I_c vs annealing time for 8 T and the annealing temperature as parameter

Figure 17 on page 23: I_c vs annealing time for 9 T and the annealing temperature as parameter

Figure 18 on page 24: I_c vs annealing time for 10 T and the annealing temperature as parameter

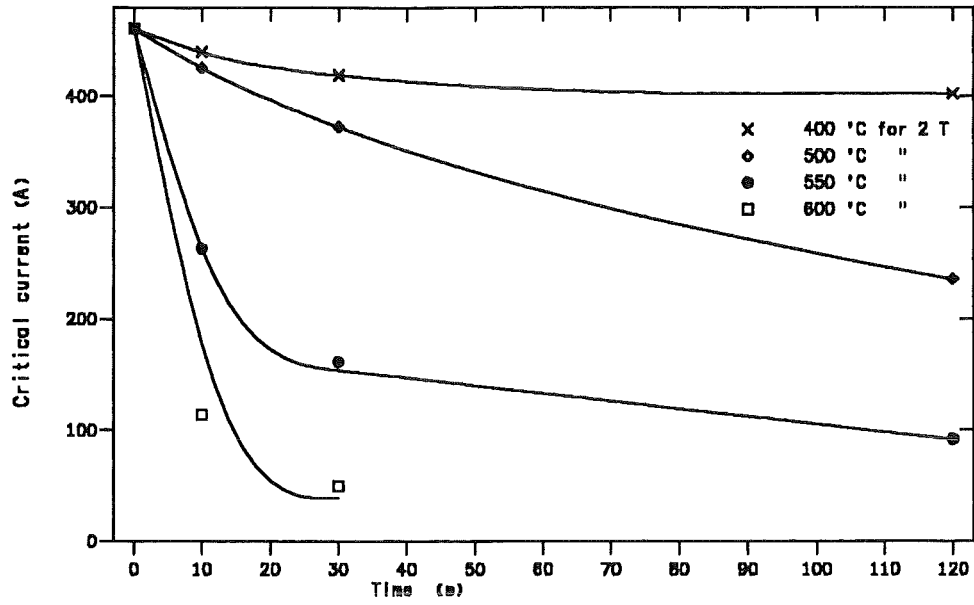


Figure 10. Characteristic current vs annealing time for 2 T. and the annealing temperature as parameter

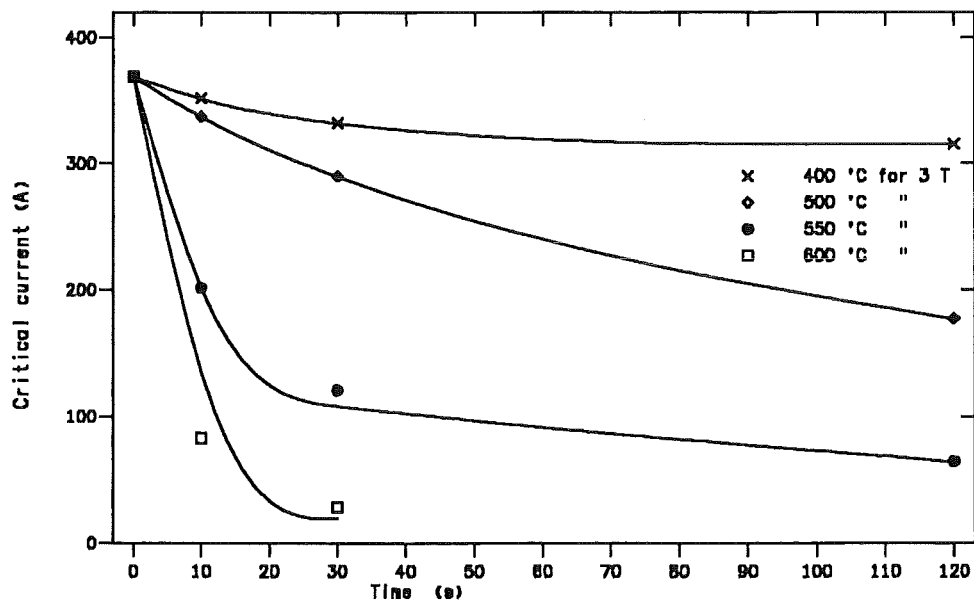


Figure 11. Characteristic current vs annealing time for 3 T. and the annealing temperature as parameter

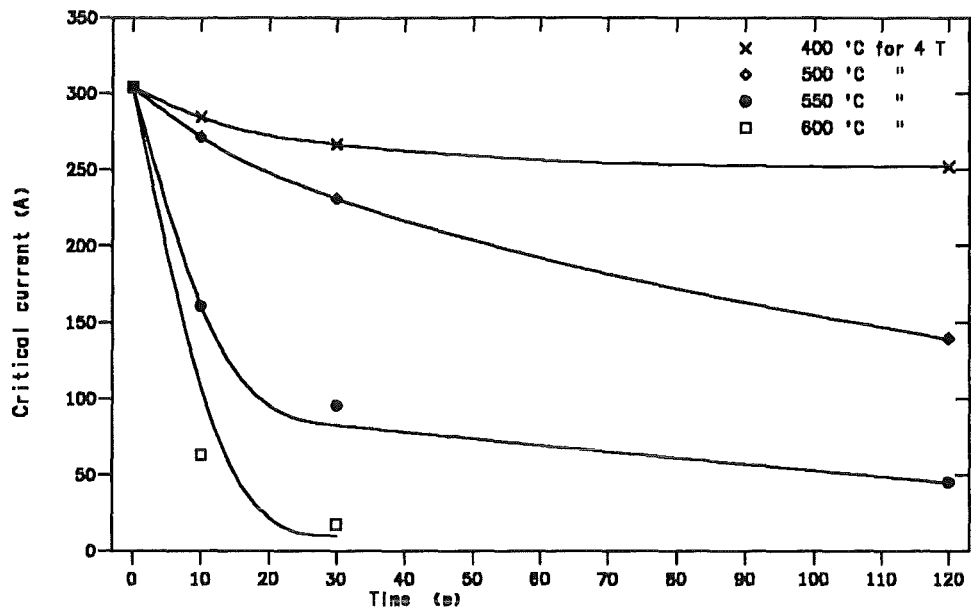


Figure 12. Characteristic current vs annealing time for 4 T. and the annealing temperature as parameter

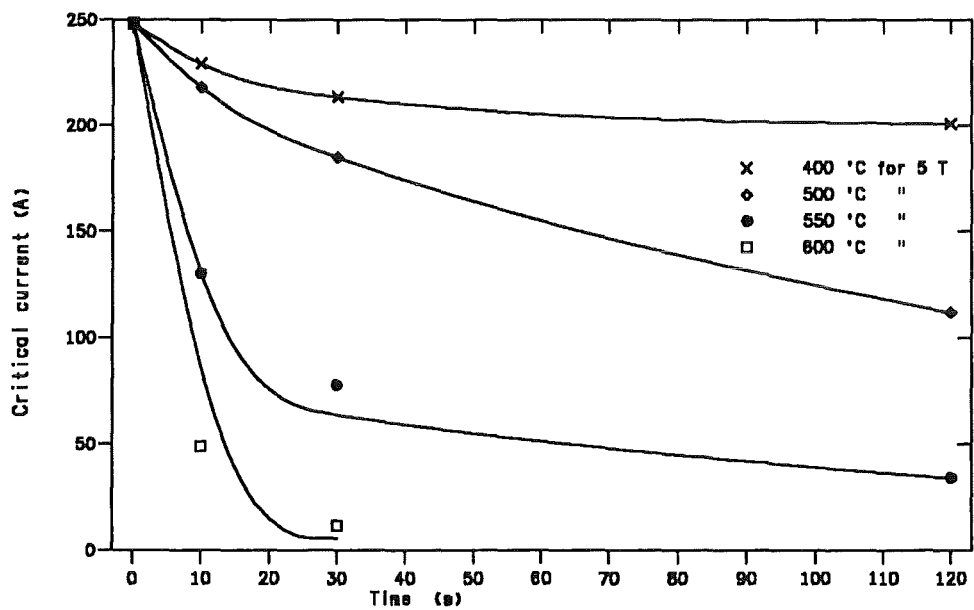


Figure 13. Characteristic current vs annealing time for 5 T. and the annealing temperature as parameter

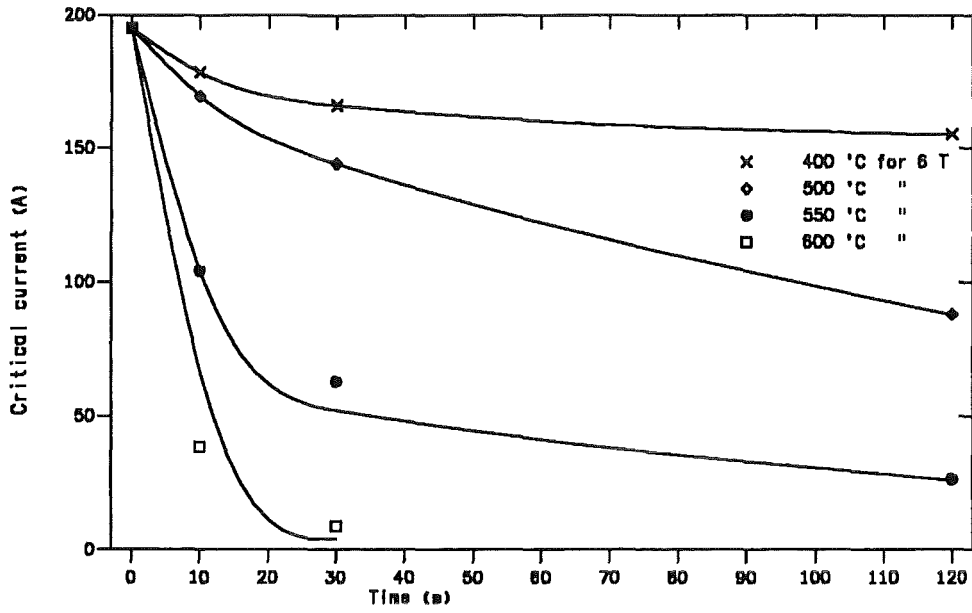


Figure 14. Characteristic current vs annealing time for 6 T. and the annealing temperature as parameter

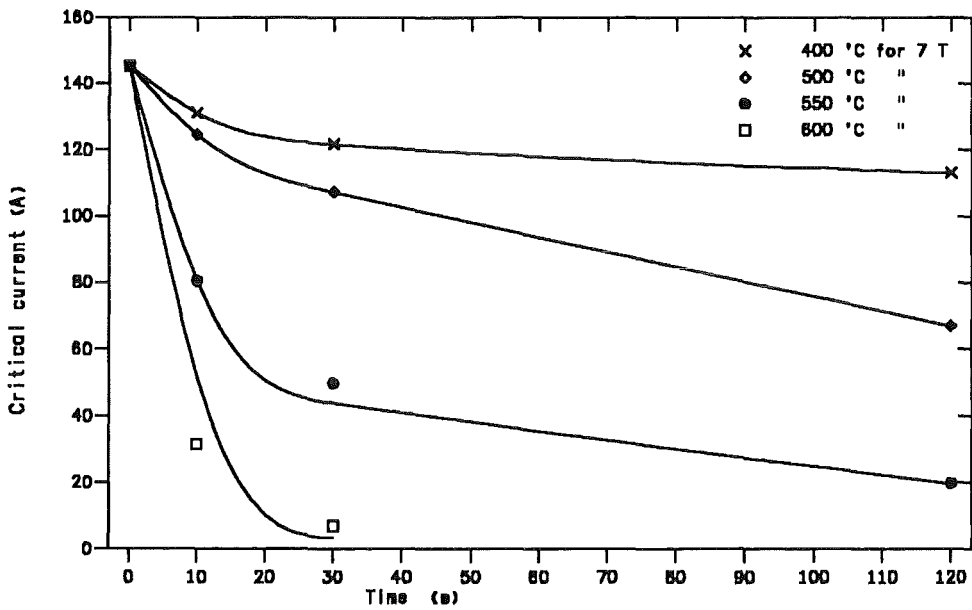


Figure 15. Characteristic current vs annealing time for 7 T. and the annealing temperature as parameter

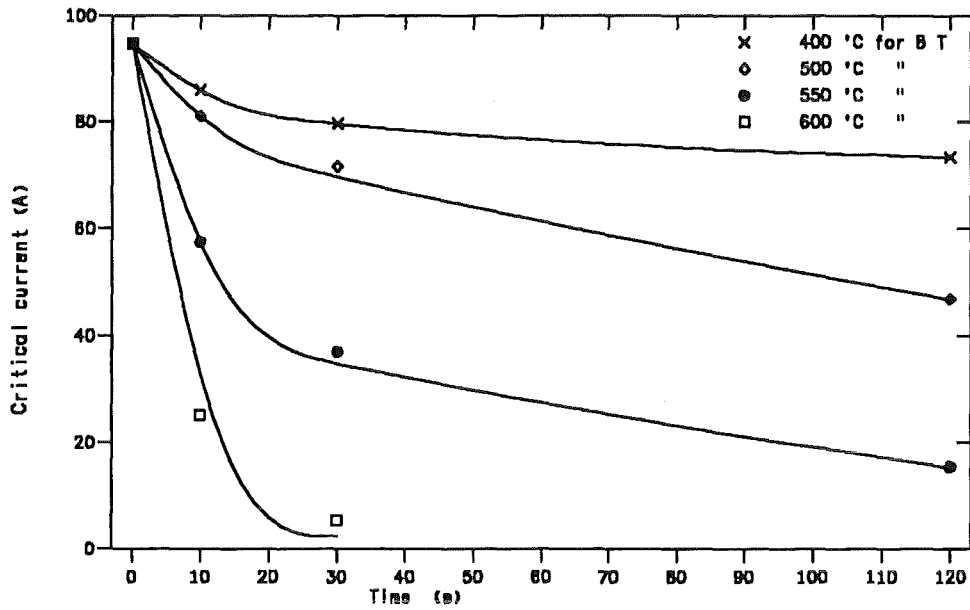


Figure 16. Characteristic current vs annealing time for 8 T. and the annealing temperature as parameter

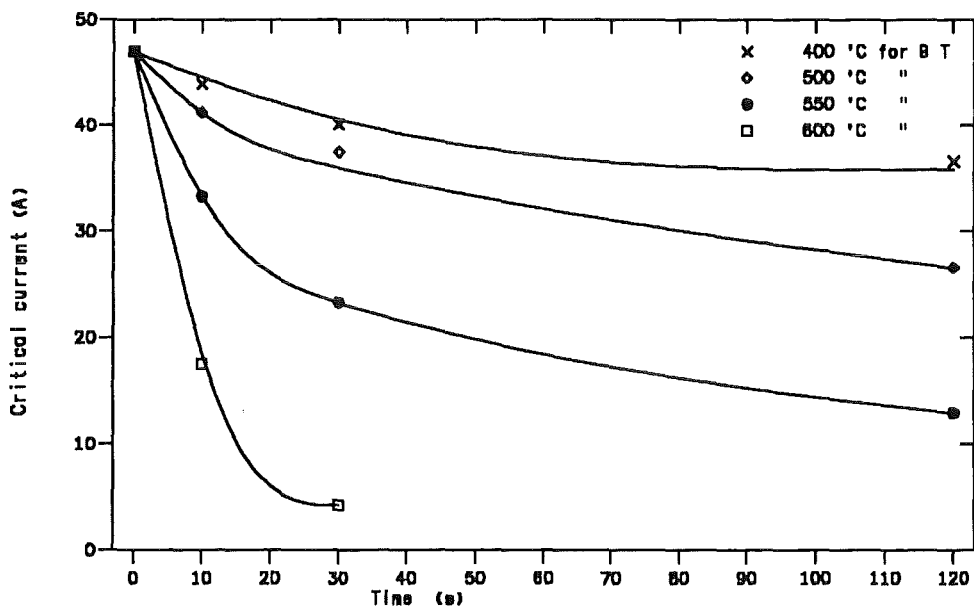


Figure 17. Characteristic current vs annealing time for 9 T. and the annealing temperature as parameter

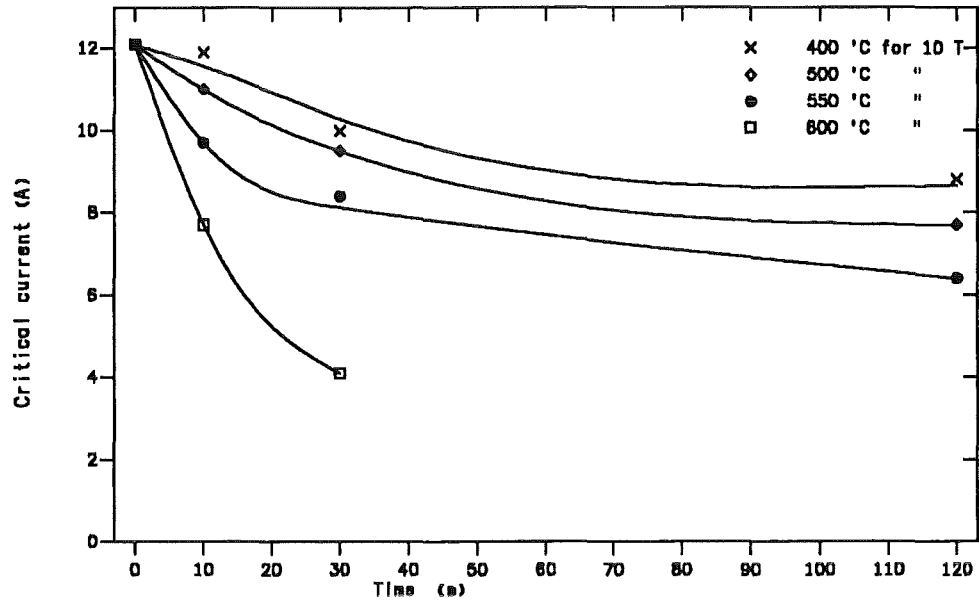


Figure 18. Characteristic current vs annealing time for 10 T. and the annealing temperature as parameter

Figures of group 4

To group 4:

Figure 19 on page 26: I_c vs annealing temperature for 2 T and the annealing time as parameter

Figure 20 on page 26: I_c vs annealing temperature for 3 T and the annealing time as parameter

Figure 21 on page 27: I_c vs annealing temperature for 4 T and the annealing time as parameter

Figure 22 on page 27: I_c vs annealing temperature for 5 T and the annealing time as parameter

Figure 23 on page 28: I_c vs annealing temperature for 6 T and the annealing time as parameter

Figure 24 on page 28: I_c vs annealing temperature for 7 T and the annealing time as parameter

Figure 25 on page 29: I_c vs annealing temperature for 8 T and the annealing time as parameter

Figure 26 on page 29: I_c vs annealing temperature for 9 T and the annealing time as parameter

Figure 27 on page 30: I_c vs annealing temperature for 10 T and the annealing time as parameter

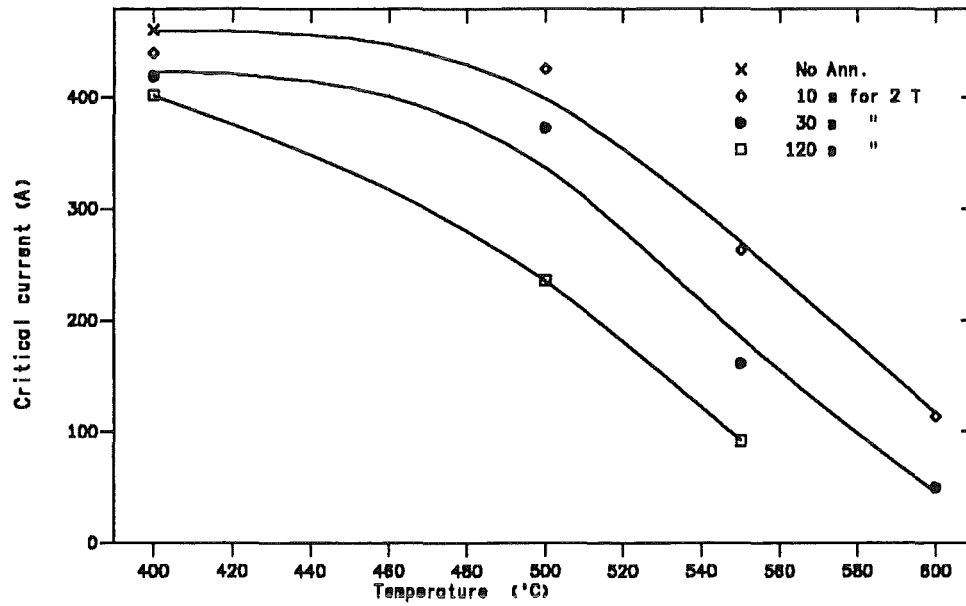


Figure 19. Characteristic current vs annealing temperature for 2 T. and the annealing time as parameter

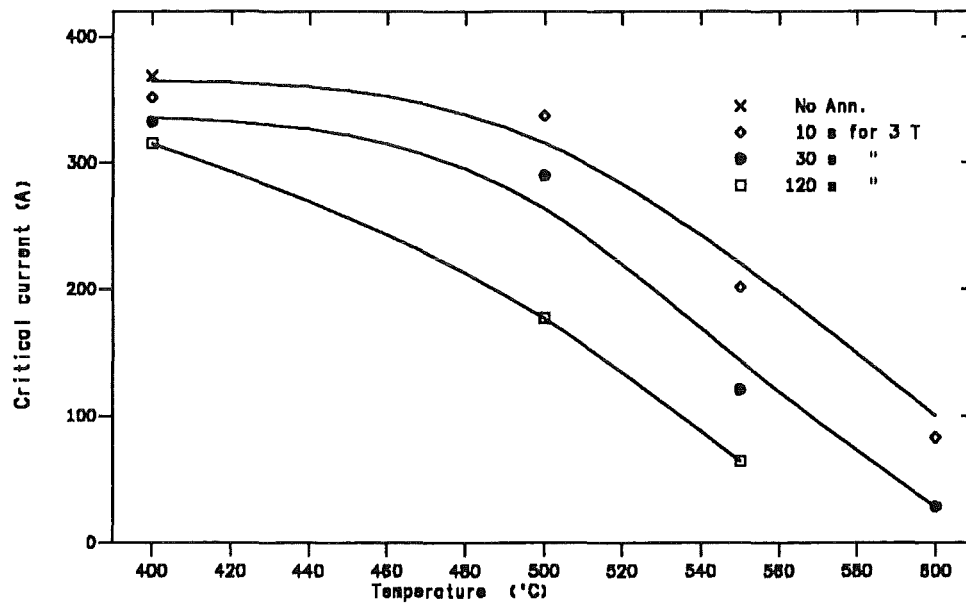


Figure 20. Characteristic current vs annealing temperature for 3 T. and the annealing time as parameter

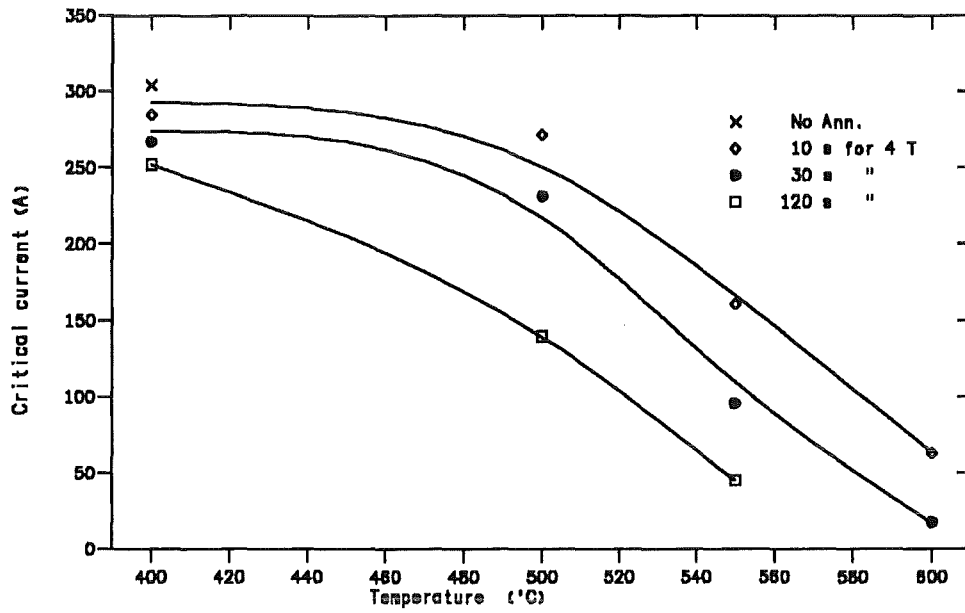


Figure 21. Characteristic current vs annealing temperature for 4 T. and the annealing time as parameter

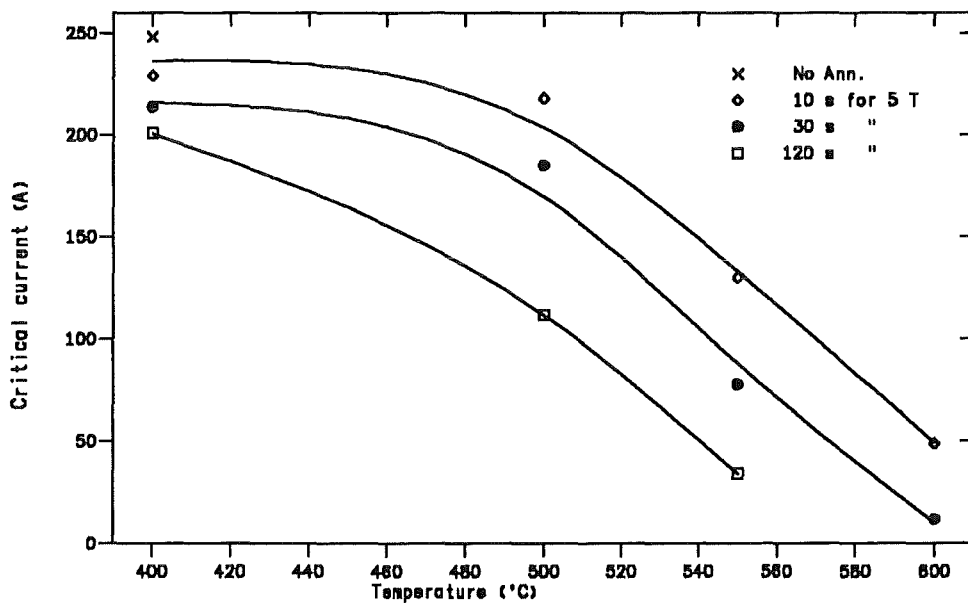


Figure 22. Characteristic current vs annealing temperature for 5 T. and the annealing time as parameter

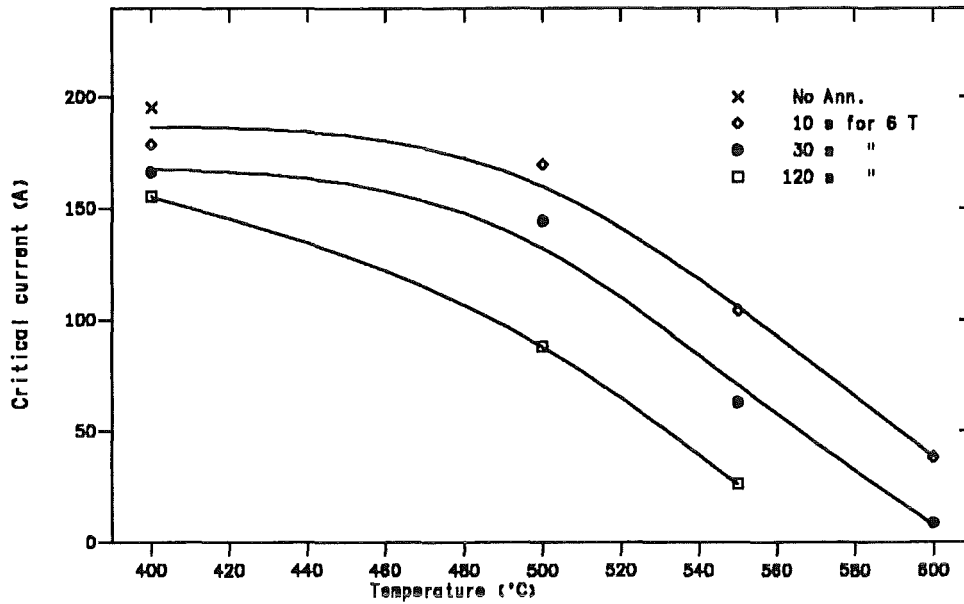


Figure 23. Characteristic current vs annealing temperature for 6 T. and the annealing time as parameter

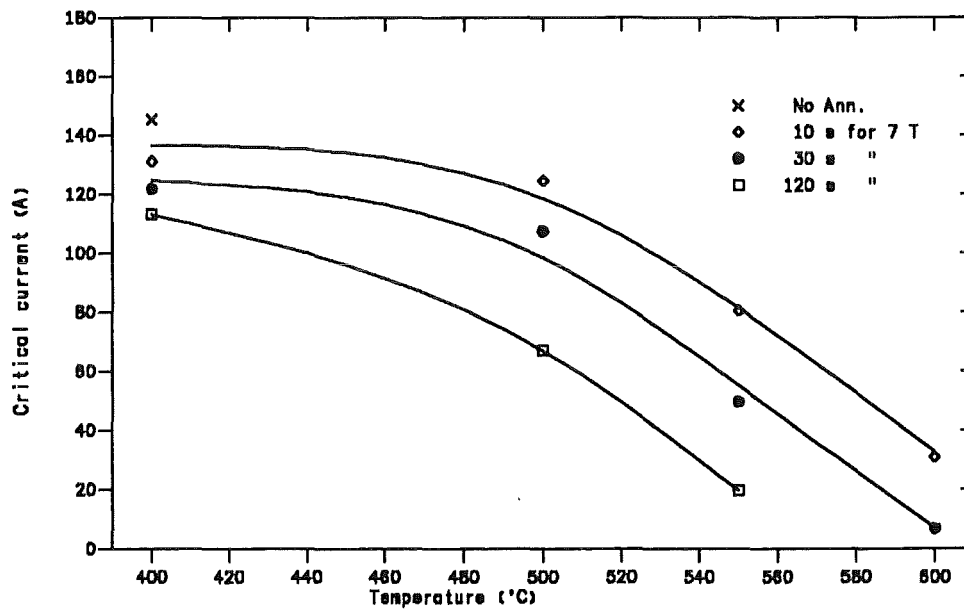


Figure 24. Characteristic current vs annealing temperature for 7 T. and the annealing time as parameter

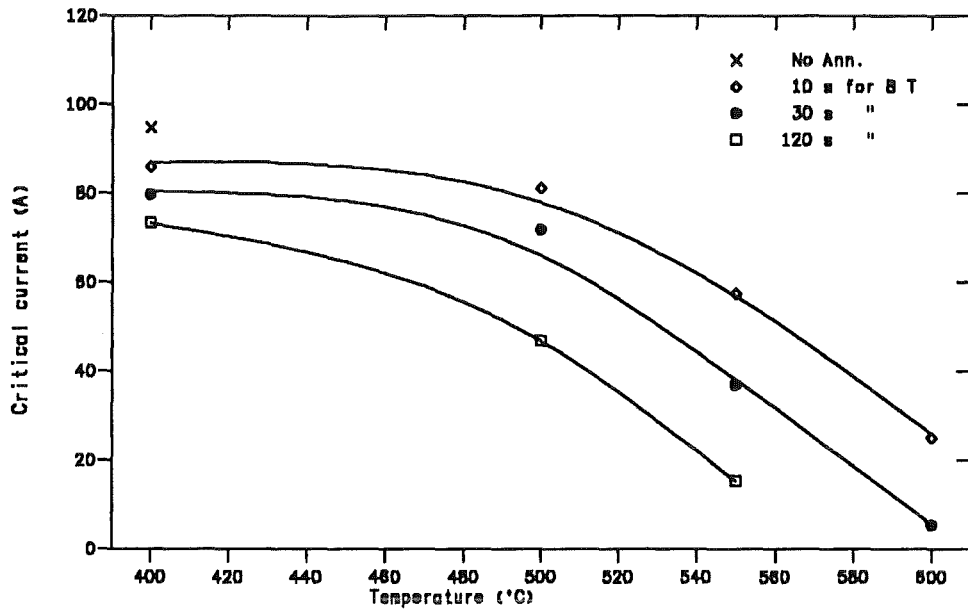


Figure 25. Characteristic current vs annealing temperature for 8 T. and the annealing time as parameter

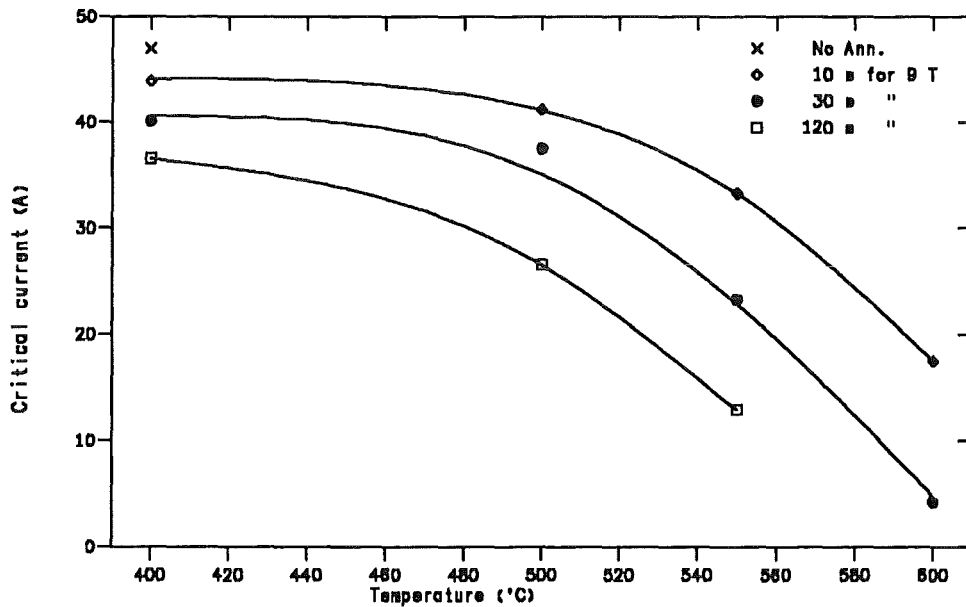


Figure 26. Characteristic current vs annealing temperature for 9 T. and the annealing time as parameter

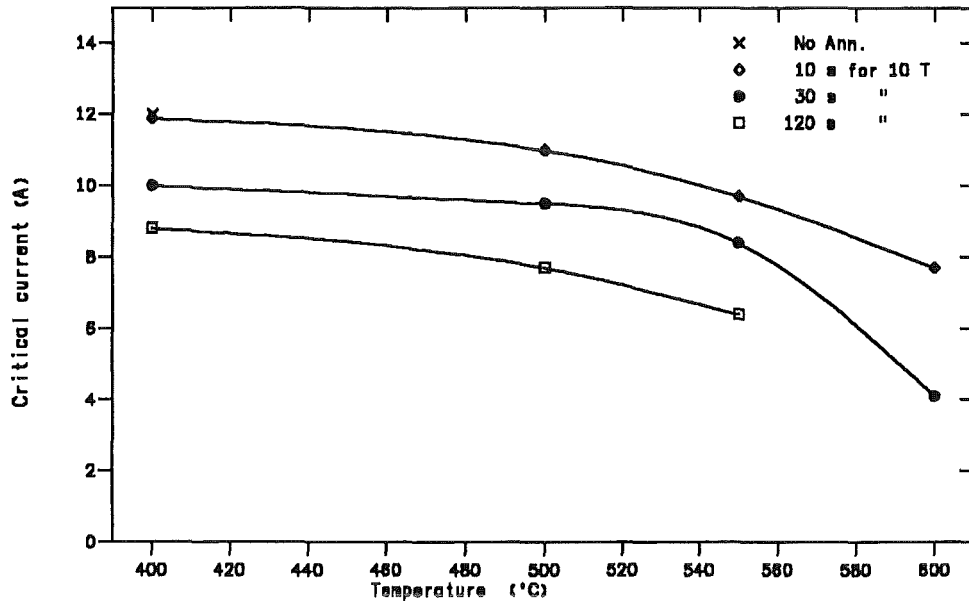


Figure 27. Characteristic current vs annealing temperature for 10 T. and the annealing time as parameter

2.6 Generalization

In order to interpret the test results and to find a general behaviour, the previous Table 5 on page 10 is translated into normalized values. The following Table 6 on page 32 shows all the values as overview. This procedure must not be over-estimated since other commercial superconducting strands are optimized in another way (e.g., for low or high field) but, in general, a tendency can be seen. However, the measurement must be repeated in each special case to get the correct absolute values.

The table is self-explaining. It shows clearly the disaster at temperatures beyond 550 °C even for an annealing time of only 10 s. In general, the TCCC is less than 30 % compared to the original ones. Also 500 °C and 30 s annealing time show a non-tolerable degradation of more than 50 % of the TCCC.

For estimation of a general tendency two kinds of figure groups are interesting:

A. Normalized current vs annealing time for a certain annealing temperature with the magnetic field as parameter

B. Normalized current vs annealing temperature for a certain annealing time with the magnetic field as parameter

The following three pictures after the table belong to the **group A**:

Figure 28 on page 33: Normalized current vs annealing time for an annealing temperature of 400 °C with the magnetic field as parameter

Figure 29 on page 33: Normalized current vs annealing time for an annealing temperature of 500 °C with the magnetic field as parameter

Figure 30 on page 34: Normalized current vs annealing time for an annealing temperature of 550 °C with the magnetic field as parameter

No picture is drawn for an annealing temperature of 600 °C due to the too low values for the current.

Table 6. Normalized characteristic current of all samples													
Characteristic current $I_{ca}(B)$ at annealing temperature and time normalized to the value $I_{c0}(B)$ without annealing													
Annealing temperature →		400 °C			500 °C			550 °C			600 °C		
Annealing time →		10 s	30 s	120 s	10 s	30 s	120 s	10 s	30 s	120 s	10 s	30 s	120 s
B [T]	No an-nealing												
2	1.0	0.954	0.909	0.872	0.923	0.808	0.511	0.571	0.35	0.199	0.247	0.108	-
3	1.0	0.953	0.901	0.854	0.914	0.785	0.48	0.546	0.327	0.175	0.225	0.077	-
4	1.0	0.936	0.877	0.828	0.893	0.761	0.459	0.529	0.315	0.149	0.208	0.058	-
5	1.0	0.923	0.86	0.809	0.878	0.745	0.45	0.524	0.313	0.138	0.197	0.048	-
6	1.0	0.915	0.851	0.796	0.869	0.739	0.451	0.534	0.322	0.135	0.197	0.045	-
7	1.0	0.902	0.838	0.779	0.857	0.739	0.461	0.554	0.342	0.136	0.215	0.047	-
8	1.0	0.908	0.842	0.775	0.856	0.757	0.495	0.607	0.391	0.163	0.265	0.057	-
9	1.0	0.934	0.853	0.779	0.877	0.798	0.566	0.709	0.496	0.274	0.372	0.089	-
10	1.0	0.983	0.826	0.727	0.909	0.785	0.636	0.802	0.694	0.529	0.636	0.339	-

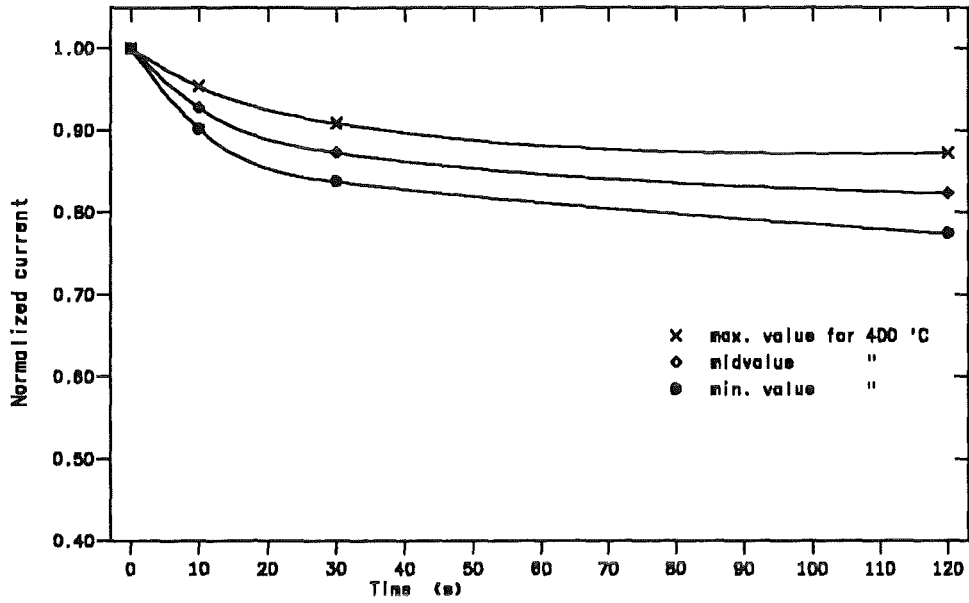


Figure 28. Normalized current vs annealing time. for an annealing temperature of 400 °C with the magnetic field as parameter

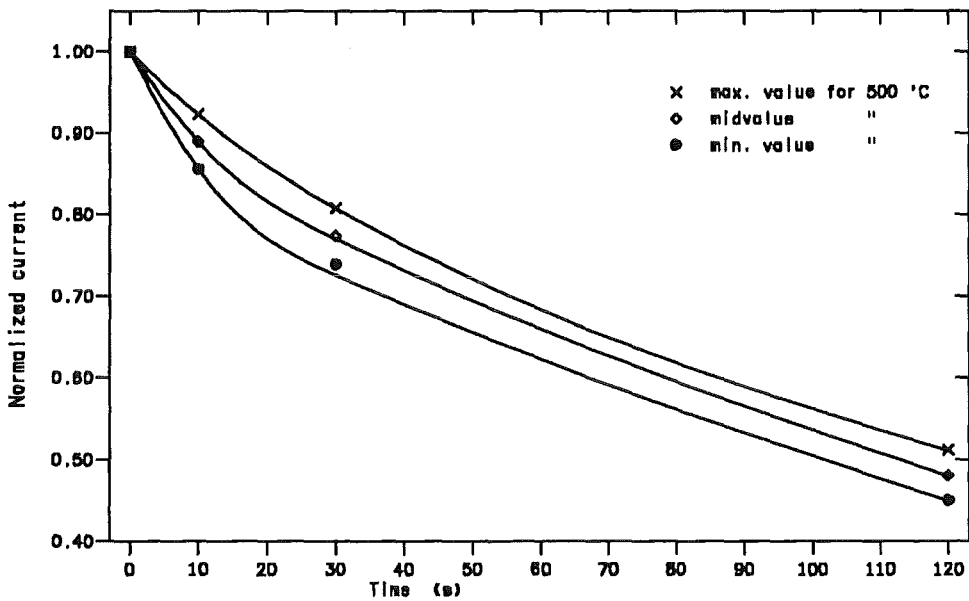


Figure 29. Normalized current vs annealing time. for an annealing temperature of 500 °C with the magnetic field as parameter

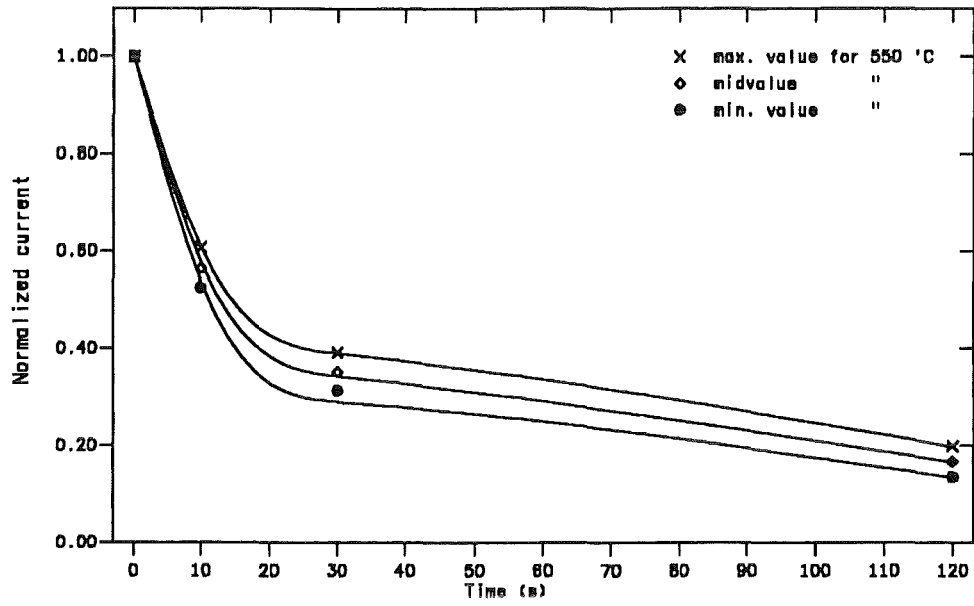


Figure 30. Normalized current vs annealing time. for an annealing temperature of 550 °C with the magnetic field as parameter

The following three pictures belong to the **group B**:

Figure 31 on page 36: Normalized current vs annealing temperature for an annealing time of 10 s with the magnetic field as parameter

Figure 32 on page 36: Normalized current vs annealing temperature for an annealing time of 30 s with the magnetic field as parameter

Figure 33 on page 37: Normalized current vs annealing temperature for an annealing time of 120 s with the magnetic field as parameter

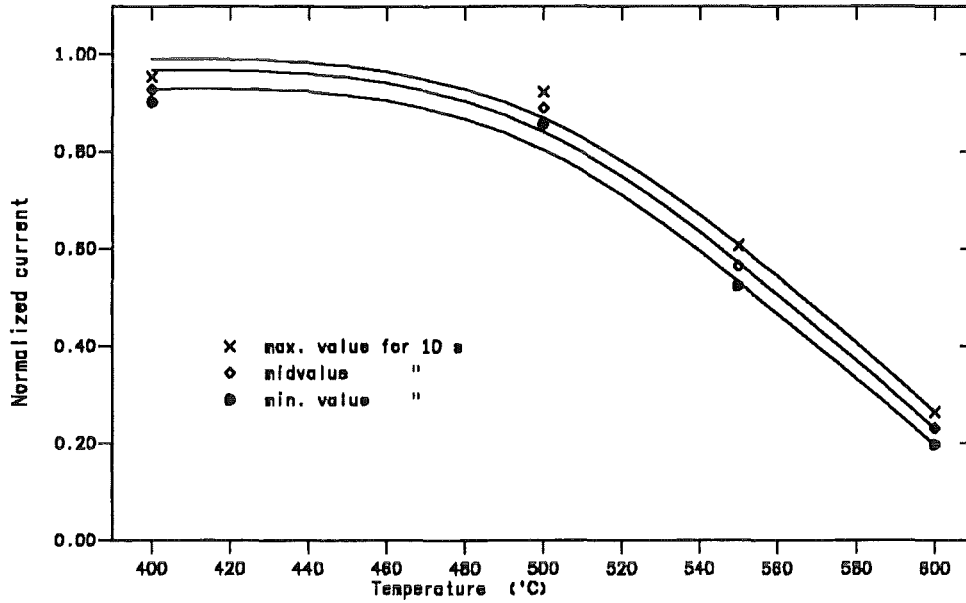


Figure 31. Normalized current vs annealing temperature. for an annealing time of 10 s with the magnetic field as parameter

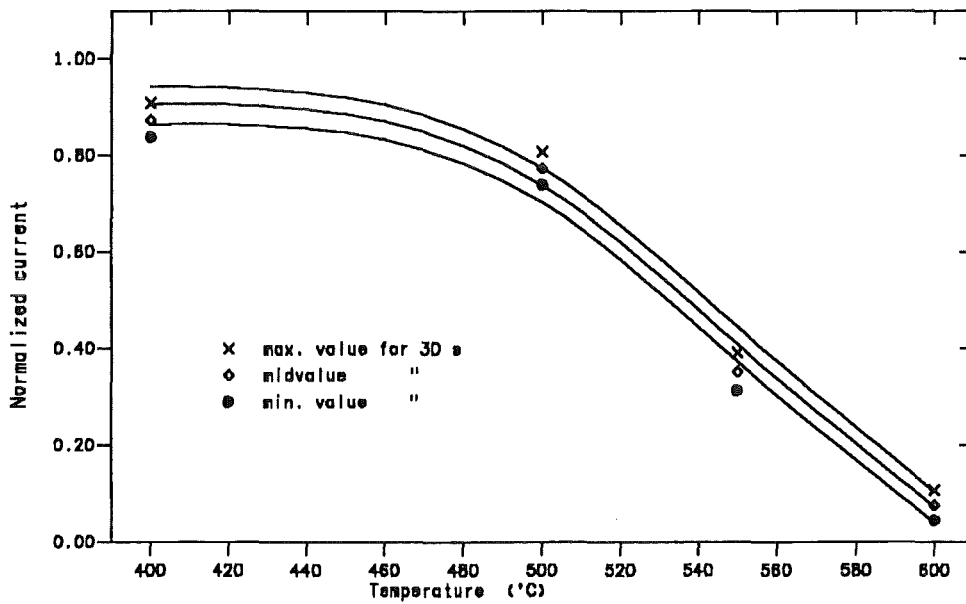


Figure 32. Normalized current vs annealing temperature. for an annealing time of 30 s with the magnetic field as parameter

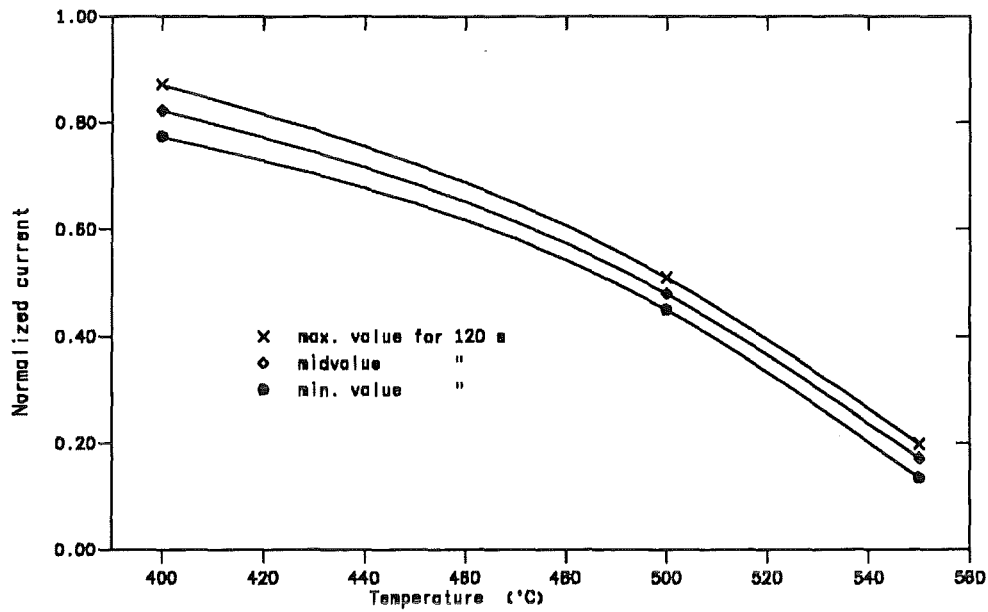


Figure 33. Normalized current vs annealing temperature. for an annealing time of 120 s with the magnetic field as parameter

3. Application to the W 7-X conductor cable

As already mentioned in the introduction, a special conductor was developed for W 7-X. This conductor is already fabricated in several hundreds of meters by LMI, Italy, and also by Noell, Germany. Both conductors are very similar.

3.1 Description of superconductor

In order to fulfil a good windability, e.g., the required minimum bending radius is only 20 cm, the technical superconductor consists of a forced flow cooled NbTi/Cu cable within an aluminium alloy conduit. The staged cable (3 x 4 x 4 x 4) is fabricated from commercially available strands. The aluminium jacket is co-extruded around the cable and is relatively soft during the three-dimensional winding process. Afterwards it is subsequently hardened to meet the mechanical requirements. Table 7 contains the main characteristics of the LMI superconductor according to [25] and additional information [26].

Table 7. Characteristic data of the LMI superconductor [25]	
Parameter	Values
Manufacturer	EM-LMI, Italy
Basic strand	Cu/Nb-Ti
Diameter of strand	0.55 mm
Matrix material	Cu
Ratio Cu/NbTi	2 : 1
RRR	> 180
Filament number	132
Filament diameter	$\leq 27 \mu\text{m}$
Twist pitch length	20 mm
Number of Sc strands	192
Cabling sequence	3 x 4 x 4 x 4
Jacket material	Al 6060T6-AlMgSi1
RRR of jacket material	2.8
Solution heat treatment temperature	$\sim 525^\circ\text{C}$.
External jacket dimension	13.8 mm x 13.8 mm (14.8 mm x 14.8 mm)
Internal jacket dimension	$\varnothing 10 \text{ mm}$
Void fraction	40 %
Critical current at 6.2 T and 4.2 K	32.8 kA
Critical current density at 6.2 T and 4.2 K	2150 A/mm ²

Figure 34 on page 40 shows the cross section of the technical superconductor for W 7-X; the left side and the centre show the complete conductor, the right side the strand.

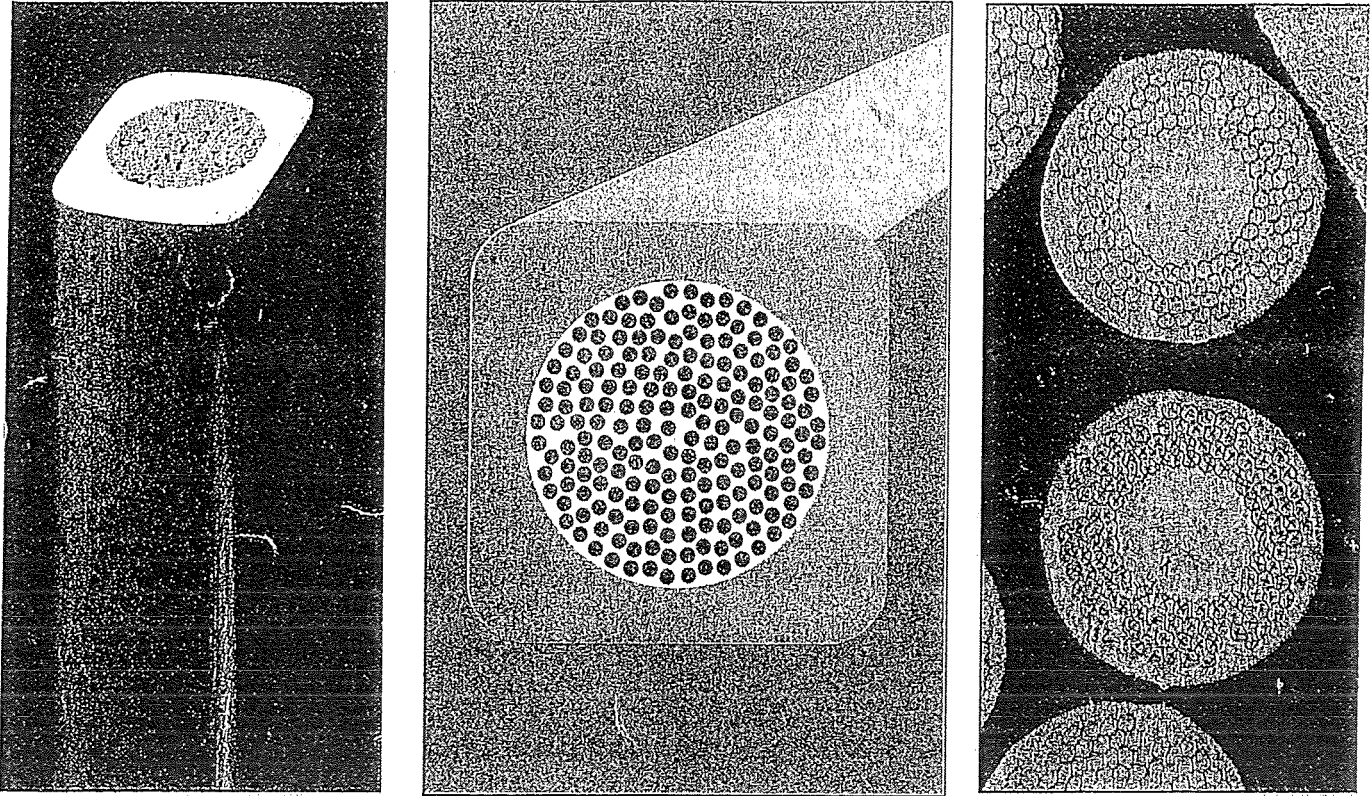


Figure 34. Technical superconductor (LMI) for W 7-X. (Right side: cross section of the strand, left side and centre: complete conductor)

3.2 Application to the W 7-X conductor cable

EM-LMI reports 2 - 10 % degradation for 500°C/30 s heat treatment and 28 - 30 % for 500°C/60 s. For the case of 500°/30 s, the characteristic current at 6 T and 4.2 K is still > 33 kA.

According to Table 7 the critical current of the cable is 32.8 kA at 6.2 T and 4.2 K. Then, the generalized data were applied to the stellarator conductor. The result is shown in the following table.

Table 8. Application to the 16 kA cable				
Time of heat treatment	30 s		120 s	
Temperature of heat treatment (°C)	I_c (kA)	%	I_c (kA)	%
no annealing	32.8	100	32.8	100
400	27.9	85	26.1	79.6
500	24.2	74	14.8	45
550	10.9	32	4.4	13.5
600	1.5	4	-	-

These values show the sensitiveness of the characteristic current from annealing time and temperature. A consequence for the jacket fabrication of the stellarator conductor is that the heat during the extrusion process should have an influence on the superconducting strands in the cable only for a few seconds. Also the extrusion speed should be as high as possible.

4. Summary and conclusion

The transport current carrying capability of commercially available NbTi superconducting wires is optimized in a very sophisticated procedure by means of cold-work and heat treatment or (annealing). The latter is done, in general, at temperatures between about 350 and 400 °C. Once optimized, an additional heat treatment, however, or an unintentional overheating influences the superconducting current carrying capability. In general, it degrades.

The cable-in-conduit superconductor for W 7-X consists of a cable with superconducting wires and a co-extruded jacket out of an Aluminium alloy for mechanical stability. This alloy must be co-extruded at a temperature > 500 °C. Therefore, a degradation of the characteristic current capability of the superconducting NbTi cable is expected.

In the investigation performed, the results of the annealing behaviour of a commercially available superconducting wire (or strand) are presented and discussed. The experimental parameters are:

Annealing temperatures: 400 °C, 500 °C, 550 °C, 600 °C

Annealing times: 10 s, 30 s, 120 s

Measurement temperature: 4.2 K

Magnetic field: up to 10 T

The results of the $I_c(B)$ measurements for the parameters annealing time and temperature are presented in tables and figures in different kinds of presentation in order to stress the tendencies of the behaviour.

Several conclusions can be drawn:

1. The degradation of the characteristic current of a NbTi multifilament conductor for temperatures less than 400 °C and times less than 30 s is tolerable for all magnetic fields. This degradation should be taken into account during design.
2. The results of the measurement in Table 5 show clearly a very strong degradation at an annealing temperature of 600 °C. The current degradation is about 75% for an annealing time of only 10 s and about 90% for 30 s. Therefore, 600 °C is not tolerable at all.
3. The results of I_c vs B for a certain annealing temperature and the annealing time as parameter show a strong **enhancement of the degradation** with rising annealing temperature for all magnetic fields. At the extrusion process, the speed should be high and the conductor should be quenched (in this case: quenched means here very fast cool down).
4. The results of I_c vs B for a certain annealing time and the annealing temperature as parameter show a strong **acceleration of the degrada-**

tion between the annealing temperatures 500 °C and 550 °C for all magnetic fields.

5. The results of I_c vs annealing time for a certain magnetic field and the annealing temperature as parameter show that the period of the first 30 s is unquestionably the decisive time.
6. The results of I_c vs annealing temperature for a certain magnetic field and the annealing time as parameter show again that the **the degradation** is accelerated between the annealing temperatures 500 °C and 550 °C for all magnetic fields.
7. The generalized presentation of the results can help to estimate the degradation of the superconductor for a special production process.
8. These results show that the mass production process for the W 7-X conductor requires a permanent and careful quality control especially for the extrusion process.

At the end of this summary, the results are shown in a 3-dimensional histogram for the critical current, annealing time, annealing temperature and for 2 T.

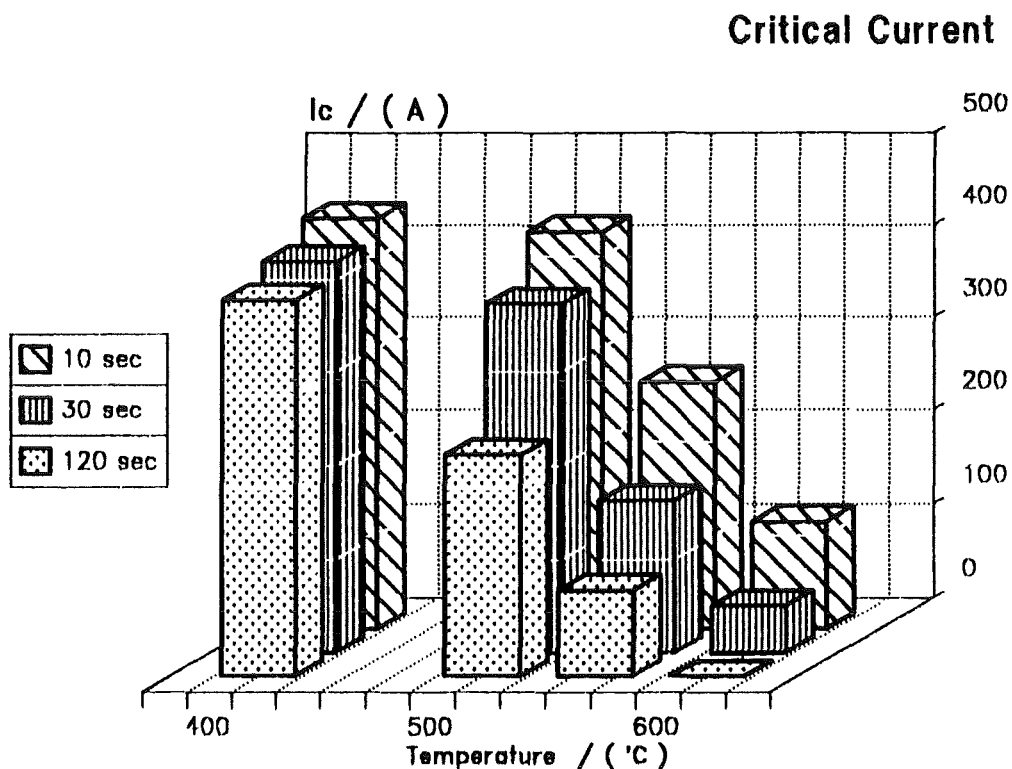


Figure 35. Histogram for the critical current, annealing time and temperature for 2T.

ACKNOWLEDGEMENTS

The authors wish to thank Mr. F. Gauland for the sample preparation and Mr. S. Stumpf for the assistance during the characteristic current measurements.

REFERENCES

- [1] C. Beidler et al., Physics and engineering design for Wendelstein 7-X, Report IPP 2/300, July 1989
- [2] R. Heller and the Wendelstein 7-X Technical Group, Superconductor for the Coils of the Modular Stellarator Wendelstein 7-X, IEEE Trans. on Magnetics, Vol.30, No. 4, July 1994, pp. 2383-2386
- [3] M.N. Wilson, Practical superconducting materials, in *Superconductors Materials Science*, edited by S. Foner, B.B. Schwartz, Plenum Press, New York (1981), 63
- [4] D.C. Larbalestier, Niobium-Titanium superconducting materials, in *Superconductors Materials Science*, edited by S. Foner, B.B. Schwartz, Plenum Press, New York (1981), 133
- [5] D.C. Larbalestier, Superconducting materials - A review of recent advances and current problems in practical materials, IEEE Trans. on Magnetics, Vol. MAG-17, No. 5, September 1981, pp. 1668-1686
- [6] A. Hillmann, Fabrication technology of superconducting materials, in *Superconductors Materials Science*, edited by S. Foner, B.B. Schwartz, Plenum Press, New York (1981), 275
- [7] H. Hillmann, Large scale fabrication of superconductors, IEEE Trans. on Magnetics, Vol. MAG-17, No. 5, September 1981, pp. 1614-1621
- [8] H. Krauth, Recent developments in NbTi superconductors at Vacuumschmelze, IEEE Trans. on Magn., VOL. 24, NO. 2, March 1988, pp. 1023-1028
- [9] G.K. Zelenskiy et al., Influence of thermomechanical working schedules on critical current density and structure of superconductor Nb-Ti base alloy, 11th Int. Conf. on Magnet Techn. (MT11), Tsukuba, Japan, 1989, pp. 604-609
- [10] J.A. Parrell, P.J. Lee, and D.C. Larbalestier, Cold work loss during heat treatment and extrusion of Nb-46.5wt%Ti composites as measured by microhardness, IEEE Trans. on Applied Superconductivity, Vol. 3, No. 1, March 1993. pp. 734-737
- [11] S. Shimamoto and H. Nomura, A new aluminium stabilized superconducting wire, Cryogenics, Aug. 1971, pp. 303-304
- [12] H. Nomura, M. Obata, and S. Shimamoto, Construction of a solenoid magnet with a new aluminium stabilized superconductor, Cryogenics, Oct. 1971, pp. 396-401
- [13] F. Wittgenstein, Detector magnets for High-Energy physics, IEEE Trans. on Magn., VOL. 28, NO. 1, January 1992, pp. 105-112
- [14] M. Thöner, Superconductors for accelerators and detectors in *New Techniques for Future Accelerators*, edited by G. Torelli, Plenum Press, New York, 1990, pp. 195-200

- [15] Y. Furuto, An overview of practical superconductor development in Japan, *Advances in Cryogenic Eng.*, Vol. 30, Plenum Press, New York and London, 1984, pp. 721-737
- [16] O. Motojima, LHD magnet system design and construction, Eleventh Topical Meeting on the Technology of Fusion Energy, New Orleans, LA, U.S.A. June 19-23, 1994
- [17] E. Baynham et al., The Aluminium stabilized superconductor for the DELPHI magnet, *Proc. of the Int. Conf. on Magnet Techn.*, Zürich, Switzerland, Sept. 9-13, 1985, pp. 639-642
- [18] R. K. Maix, D. Salathé, Practical scaling formulas for the determination of critical currents of NbTi superconductors, *Proc. of the Int. Conf. on Magnet Techn.*, Zürich, Switzerland, Sept. 9-13, 1985, pp. 535-538
- [19] J. Le Bars et al., An Aluminum stabilized conductor for the ALEPH Solenoid, *IEEE Trans. Magn.*, VOL. MAG-23, NO. 2, March 1987, pp. 1444-1447
- [20] R. Bruzzese et al., The Aluminum stabilized Nb-Ti conductor for the ZEUS thin solenoid, *IEEE Trans. Magn.*, Vol. 25, March 1989, pp. 1827-1830
- [21] H. C. Kanithi, D. Phillips, C. King, and B.A. Zeitlin, Development and Characterization of Aluminum Clad Superconductors, *IEEE Trans. on Magn.*, VOL. 24, NO. 2, March 1988, pp. 1029-1032
- [22] H. C. Kanithi, D. Phillips, and B.A. Zeitlin, Further Development of Aluminum Clad Superconductors, *IEEE Trans. on Magn.*, VOL. 27, NO. 2, March 1991, pp. 1803-1806
- [23] Th. Schneider, P. Turowski, Critical current degradation of a NbTi-multifilament conductor due to heat treatment, *IEEE Trans. on Magnetics*, Vol.30, No. 4, July 1994, pp. 2391-2394
- [24] Swissmetal Dornach, Superconductor Data Sheet S-48
- [25] EUROPA METALLI-LMI spa, Superconductor Data Sheet: ALUMINIUM ALLOY JACKETED CABLE IN CONDUIT
- [26] M. Pillsticker, IPP, private communication, July 1994